INVESTIGATION OF MULTIPHASE METERING SYSTEMS AND MEASURING ACCURACY IN BIBIYANA GAS FIELD

MD. EMDADUL HAQUE

DEPARTMENT OF PETROLEUM & MINERAL RESOURCES ENGINEERING

BUET, DHAKA, BANGLADESH

APRIL 2013

INVESTIGATION OF MULTIPHASE METERING SYSTEMS AND MEASURING ACCURACY IN BIBIYANA GAS FIELD

A Project

Submitted to the Department of Petroleum & Mineral Resources Engineering

in partial fulfillment of the requirements for the

Degree of Master of Engineering (Petroleum)

By

MD. EMDADUL HAQUE

DEPARTMENT OF PETROLEUM & MINERAL RESOURCES ENGINEERING

BUET, DHAKA, BANGLADESH

APRIL 2013

CANDIDATE'S DECLARATION

It is hereby declared that this project or any part of it has not been submitted elsewhere for the award of any degree or diploma.

Signature of the Candidate

……………………………….

(Md. Emdadul Haque)

RECOMMENDATION OF THE BOARD OF EXAMINERS

The undersigned certify that they have read and recommended to the department of Petroleum and Mineral Resources Engineering, for acceptance, a project entitled “INVESTIGATION OF MULTIPHASE METERING SYSTEMS AND MEASURING ACCURACY IN BIBIYANA GAS FIELD”submitted by MD. EMDADUL HAQUE in partial fulfillment of the requirements for the degree of MASTER OF ENGINEERING in PETROLEUM ENGINEERING.

Chairman (Supervisor) :________________________________

Dr. Mohammad Tamim
Professor,
Dept. of Petroleum & Mineral Resources Engineering,
BUET

Member :________________________________

Dr. Mohammed Mahbubur Rahman
Associate Professor,
Dept. of Petroleum & Mineral Resources Engineering,
BUET

Member :________________________________

Dr. Ijaz Hossain
Professor,
Dept. of Chemical Engineering,
BUET

29th APRIL 2013

DEDICATED TO MY BELOVED PARENTS AND RESPECTED TEACHERS OF PETROLEUM ENGINEERING DEPARTMENT

ACKNOWLEDGEMENT

I would like to express my appreciation to a number of individuals who helped producing this work. First and foremost my appreciation is extended to my project supervisor Dr. Mohammad Tamim, Professor, PMRE, BUET, for his valuable guidance and supervision throughout the entire project work. I would like to express my sincere gratitude for his patience and encouragement throughout this work, without which this work would not have been possible.

I am ever grateful to Mohammad Mozammel Huque, Assistant Professor, PMRE, BUET, for his support to carry out this project. I am grateful to Dr. Mohammed Mahbubur Rahman, Associate Professor, PMRE, BUET and Dr. Ijaz Hossain, Professor, Department of Chemical Engineering, BUET, for their valuable time as the examiners of the report and their insightful ideas and suggestions.

I am pleased to the entire Petroleum Engineering Department, BUET for their significant contribution to my academic and intellectual development. I firmly believe that they have enriched me as a petroleum engineer and I will carry with me the skills they have given in my future work.

I would like to thank my colleagues in Bibiyana Gas Plant for their suggestions and support to carry out this work.

ABSTRACT

The Bibiyana gas field is the second largest gas field in Bangladesh, it has started its production on March 2007. Now it is producing about 840 MMSCF Gas and 3500 bbls condensate each day from 12 producing wells. All producing wells are located in two regions, such as North Pad and South Pad. In south pad 5 wells and gas processing facilities are situated and in North pad remaining 7 wells are located and connected to south pad process plant via common production header. Each well of North pad are comprised of individual Multiphase Flow Meter instead of conventional Test Separator system. Bibiyana Gas Filed first introduced this type of flow meter in Bangladesh to achieve better surveillance of reservoir and to apply better production allocation. Due to wrong selection of meter, fluid flow regime mismatch and due to lack of proper fluid sampling procedure this multiphase flow meter performance may also hamper. As per manufacturers' information, this flow meters accuracy is within ±5%, while in practice it is found that this error is about 6-9%. This project work determines the fluid flow profile by using Taitel-Dukler Model, investigates the working principle of this flow meter and their sampling and calibration technique. This flow meter measures gas flow rate by using v-cone differential pressure formula, water detection by microwave technology and hydrocarbon part is analyzed by PVT Software. As per equipment data sheet, it is found that this flow meter works well for Oil density 43.5~45.1 lb/ft^3 and gas density 1.15~4.46 lb/ft^3 while calculated value is approximately 47.8 lb/ft^3 for oil and 0.05 lb/ft^3 for gases. To find out the causes, this study investigates for any phase changes from well head to separator and found no phase changes occur in individual flow line for different flow rates. All calculation including fluid pattern are done manually and phase changes are investigated by HYSYS Model. Later flow accuracy is done manually by using Field

Data of the Bibiyana Gas Field. This project also analyzes the applicability and selection criteria of Multiphase Flow Meter in Bangladesh in respect to installation cost, maintenance cost, fluid property, type of meter and calibration technique. Finally this study suggests that the existing technology can be used for process parameters monitoring within limited uncertainties and not suitable for custody transfer metering.

TABLE OF CONTENTS

LIST OF FIGURES

Page

LIST OF TABLES

NOMENCLATURE

A	Annular
ACFS	Actual Cubic Feet per Second
BBLS	Barrels
BCF	Billion Cubic Feet
BPD	Barrels per Day
BTU	British Thermal Unit
BYGP	Bibiyana Gas Plant
CAPEX	Capital Expenditure
CT	Computed Tomography
EOS	Equation of State
GAP	Gathering Allocation Performance
GOR	Gas Oil Ratio
GVF	Gas Volume Fraction
I	Intermittent
IPM	Integrated Production Modeling
MFM	Multiphase Flow Meter
MMSCFD	Million Standard Cubic Feet per Day
MSCFD	Thousand Standard Cubic Feet per Day
NMR	Nuclear Magnetic Resonance
PDF	Probability Density Function
PI	Pressure Indicating Gauge

PMRE	Petroleum and Mineral Resources Engineering
PSIA	Pounds per Square Inch in Absolute
PSIG	Pounds per Square Inch in Gauge
PVT	Pressure Volume Temperature
PVSV	Pressure/Vacuum Safety Valve
SG	Specific Gravity
SCF	Standard Cubic Feet
SCSSV	Surface Controlled Subsurface Safety Valve
SS	Stratified Smooth
SW	Stratified Wavy
RFM	Roxar Flow Meter
WC	Water Column
WGM	Wet Gas Meter

A	Area
$\tilde{A}_G$	Gas Fraction
$\tilde{A}_L$	Liquid Fraction
β	Beta Ratio
C_D	Discharge Coefficient
Cp	Specific heat capacity at constant pressure
C_v	Specific heat capacity at constant volume
D	Diameter
dP	Differential Pressure

$\left(\frac{dP}{dx}\right) gs$	Superficial Pressure Drop for Gas
$\left(\frac{dP}{dx}\right) ls$	Superficial Pressure Drop for Liquid
F_r	Froude Number
$\widetilde{h_L}$	Liquid Fraction
K	Specific Heat Ratio
L	Length
λ_L	Liquid Holdup
μ_l	Liquid Viscosity
μ_g	Gas Viscosity
μ_m	Mixture Viscosity
P	Pressure
Φ_g	Two phase multiplier
Q_g	Gas Flow Rate
$\overline{R}$	Gas constant
R	Universal gas constant
Re	Reynolds Number
$\tilde{S}_G$	Gas Slip
$\tilde{S}_L$	Liquid Slip
ρ_l	Liquid Density
ρ_g	Gas Density
ρ_m	Mixture Density
U_g	Superficial Gas Velocity

U_l	Superficial Liquid Velocity
U_m	Mixture Superficial Velocity
V	Velocity
ν	Kinematic Viscosity
X	Lockhart-Martinelli Factor
y	Fluid Expansibility Factor

Subscripts

d	Discharge
g	Gas phase
l	Liquid phase
m	Mixed Phase

Chapter 1

INTRODUCTION

1.1 Overview of Bibiyana Gas Field

The Bibiyana Gas Field is located in north-eastern part of Bangladesh in Block 12 and 150 km northeast of Dhaka. The field comprises of a North Pad and a South Pad, separated by 4.5 km. There are 7 producing wells in the North Pad and 5 in the South Pad. The Gas Plant, Control Room, Sales Pipeline, and Metering Station are all located with the five wells at the South Pad. Product export from the Gas Plant is via 30” gas pipeline and 6” condensate pipeline, tied into Gas Transmission Company Limited’s (GTCL) North-South pipeline grid at Muchai Valve Station near Rashidpur, approximately 42 km south of the South Pad. This is the second largest gas field in Bangladesh, has started production on March 2007 with 200 MMSCFD. Since then it has steadily increased production every year and from February 2013, it is producing approximately 840 MMSCFD Gas and 3500 BPD condensate.

1.2 Well Arrangement

All producing wells are located in two sites; North pad and South Pad. North Pad is included 7 producing wells with 5 future connections and rest of the wells and gas processing facility are in South Pad. North Pad is included with production manifold, multiphase metering, a vent stack, the upstream terminus of a gathering pipeline including a scrapper/sphere launcher and provision for future gathering line connection. Each wellhead is included with hydraulically actuated surface controlled subsurface safety valves (SCSSV), master valve and wing valve (pneumatic). Fluid flow is controlled by remote-actuated choke valve downstream of the wing valve in each wellhead flow line. Gas downstream of this choke valve is in the mixed phase at the 1280 psig and 88°F. Individual wellhead flow lines included multiphase flow meters for tracking individual well performance and also for monitoring and control purposes. Multiple wellhead flow line segments combine into a separate production header upstream of the 4.5 km 20” gathering pipeline. The total production rate from the North Pad is designed for 300 MMSCFD of Gas. Each flow line also includes for provision for methanol injection for hydrate prevention and corrosion inhibitor injection. Rather than multiphase meter like in the North Pad, the South Pad well makeup is monitored through a Test Separator to monitor the amount of each phase present. Only one well flow line is to be aligned to the Test Separator loop at a time [1].

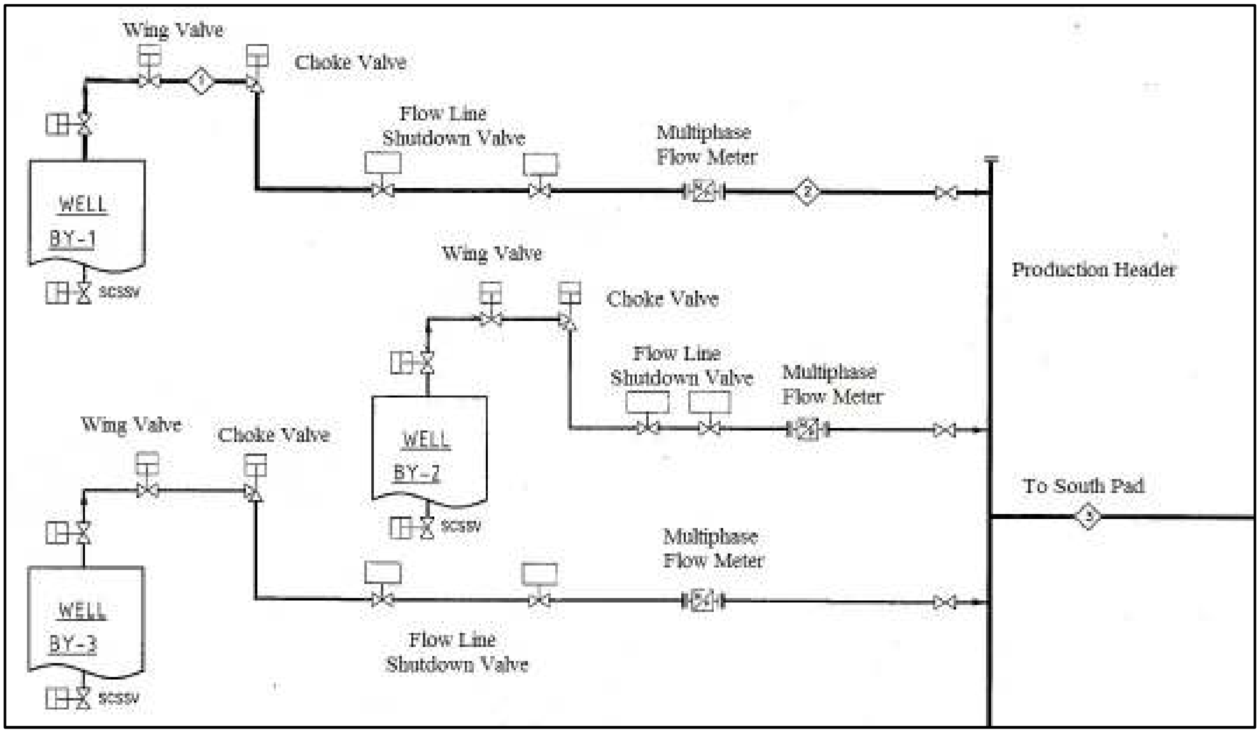

Figure 1.1 Schematic of North Pad Well Arrangement

1.3 Well Testing System

In order to optimize the production and maximize recovery from reservoir, continuous monitoring of each well is desired. Well testing at regular intervals is the current norm to understand the performance of the well. Also, well testing data is only obtained for specific time periods.

In BYGP, well test is performed in two ways:

1.3.1 Test Separator System for South Pad Wells

1.3.2 Multiphase Metering for North Pad Wells

1.3.1 Test Separator System for South Pad Wells

The stream from the well being tested is separated in three phases; typically oil, gas and water in the test separator and each phase stream are individually metered. Separate Production and Test Manifolds are installed at the South Pad. Only one well is to be lined up to the Test Manifold at a given time while the remaining wells are lined up to the Production Header. The Test Manifolds feeds a Test Separator Vessel that separates the hydrocarbon liquids, produced water and hydrocarbon gas. Test Header is equipped with Orifice, Pressure, Temperature and differential pressure transmitter and at the exit of Test Separator, Gas is measured by Orifice Meter, Condensate and Water is measured separately by Turbine Flow Meter. As per well testing schedule, one well put into Test Separator for one week, by this time Condensate and Water production is measured at fixed Gas Flow Rate, and water salinity is also tested for predicting the water production rate. Moreover, every year Bottom Hole Pressure (BHP) survey has conducted to understand the reservoir condition and well performance.

1.3.2 Multiphase Metering for North Pad Wells

There are 7 wells in the North Pad; each flow lines are equipped with Multiphase Flow Meter (MFM). The use of MFM offers online installation on flow streams which enables continuous monitoring of individual well. An important feature of this MFM is that it does not need the bulk physical separation of each phase to obtain the flow rates of each phase. MFM are also much smaller in dimensions and lower in weight as compared to test separators. Thus by using MFM in BYGP as a replacement for test separator, the high installation and operation cost, test lines, manifolds and valve systems were eliminated. The MFM can detect water content in the gas and individual flow rate of hydrocarbons and water. This is designed for the fluid where Gas Volume Fraction (GVF)>95%vol. The MFM detects the water content based on microwave technology and flow rates using a v-cone differential pressure device. The split between gas and condensate is found using PVT calculations and such the meter depends on input of the true hydrocarbon composition [2, 3].

Chapter 2

STATEMENT OF THE PROBLEM

2.1 Introduction

Multiphase Flow Meters are equipped in each flow line of North Pad Well System of BYGP. These flow meters are playing a vital role for well surveillance, well testing and production allocation. To understand reservoir behavior and optimize the production, flow accuracy of each streams are very important. This project investigated on uncertainty level of Multiphase Flow Meter data which should be within ±5% range as suggested by Manufacturer.

2.2 Flow Measurement Scenario

The Multiphase Flow Meter detects the water content based on microwave technology and flow rates using a v-cone differential pressure device. The split between gas and condensate is found using PVT calculations and such the meter depends on input of the true hydrocarbon composition. Figure 2.1 illustrates the typical arrangement of Multiphase Flow Meter.

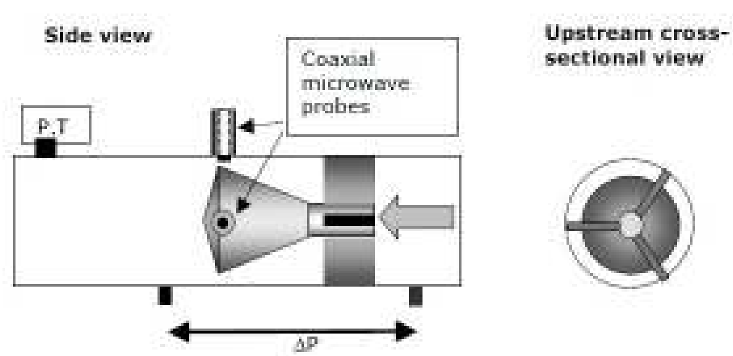

Figure 2.1 V-Cone based Wet Gas Meter [3]

2.2.1 System Components

The MFM consists of the following main parts:

- **Meter Body**
  Microwave based water fraction meter, differential pressure flow meter V-cone with ΔP Transmitter, Pressure Transmitter, Temperature Transmitter
- **Electronic Unit**
  Microwave electronics, Wet gas flow computer, Power supply unit
- **Software Unit**
  Microwave control software, wet gas flow computer software, PVT Software

The water fraction of the total volume is measured using the microwave resonator sensor, pressure transmitter, temperature transmitter and microwave control software. The split of hydrocarbons between a liquid and gas phase is calculated using a PVT Software Package and using pressure, temperature as input. The measured composition is subsequently used together with the differential pressure as input to the flow computer to calculate individual flow rates of gas, condensate and water.

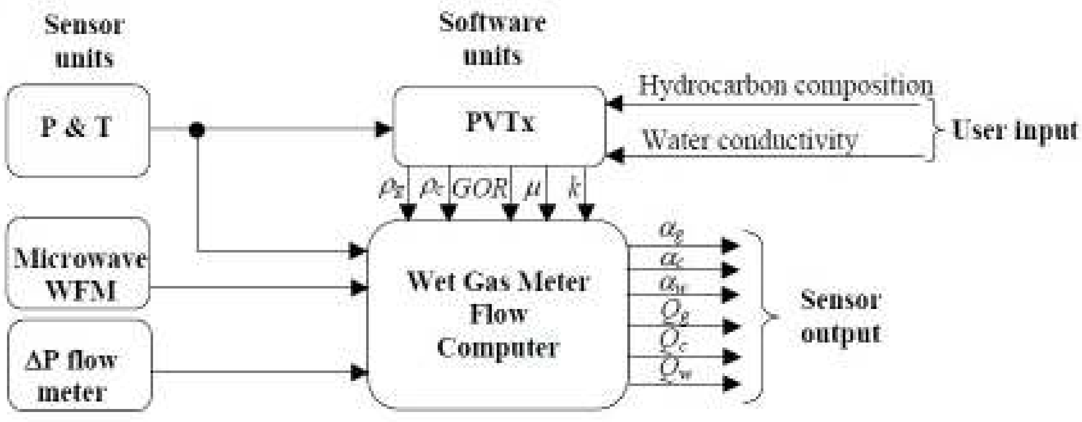

Figure 2.2 Wet Gas Meter Measurement Concept [3]

In Figure 2.2, Wet Gas Meter measurement concept has been described where hydrocarbon composition and water conductivity need to input of software unit. This software will get input of pressure and temperature from sensor, microwave intensity, pressure differential data and finally flow computer gives the output as fraction and flow rate of gas, oil and water.

2.2.2 PVT Software

A PVT Software package is integrated as part of the WGM software. PVTx is used for reservoir fluid characterization based on a cubic equation of state (EOS). It is a versatile tool for characterizing multi-component mixtures with emphasis on reservoir fluids.

Input to the PVT package is hydrocarbon composition and it is used to:

- Calculate the gas density at meter conditions and standard conditions.
- Calculate the condensate density meter conditions and standard conditions.
- Calculate the actual Gas/Oil Volume Ratio (GOR) at meter conditions and standard conditions. The calculated GOR is subsequently employed to discriminate between gas and oil/condensate and hence deduce the condensate and gas fraction, once the water fraction has been found using the WFM.

The densities and GOR at standard conditions given by the PVT package, is used to calculate the flow rates at standard conditions. It is also possible to have flow rate output at other conditions, specified by the user. The hydrocarbon composition, used as input to PVTx, of the reservoir should include the mole% of each component N_2, CO_2, H_2S, C_1, …….. upto PC_7 or PC_{10}, the data from the last components $PC_7 – PC_{10}$ should also include molecular weight and density [4].

2.3 Measurement Uncertainty

Uncertainty in flow measurement arises from the variability (or uncertainty) in one or more factors, e.g. the fluid properties, flow regime, flow rate, instrumentation, and quality of the measurement model. Multiphase flow meters measure unprocessed fluids with two or more phases simultaneously, thereby increasing the complexity of the measurement equations and model. Uncertainty in multiphase flow meters is mainly due to changes in process conditions, fluid properties, flow models, measurement devices, and sensors. The impact of these uncertainties on the uncertainty of each phase typically increases considerably as the water liquid ratio (WLR), gas volume fraction (GVF) and multiphase flow rate approach their limits. Performance based on laboratory tests, the meter data should be within following range [3, 4]:

Gas Volume Fraction (GVF) Range: 90-100%

Water Liquid Ratio (WLR) Range: 0-100% for GVF>99%

0-50% for 90% <GVF<99%

Hydrocarbon Flow Rate Accuracy:

± 3 - $4\%_{rel}$ for GVF>99%, WLR= 0-100%

± 3 - $4\%_{rel}$ for GVF<99%, WLR= 0-50%

Water detection accuracy:

$\pm 0.1\%_{abs}$ for GVF>99%, WLR= 0-100%

$\pm 0.2\%_{abs}$ for GVF<99%, WLR= 0-50%

Not specified for GVF<99%, WLR= 50-100%

Water detection sensitivity: $\pm 0.005\%_{abs}$ (50 ppm)

2.4 Objectives

- To determine the fluid flow pattern from the PVT properties.
- To verify the working principle of existing multiphase meter with reservoir fluid properties.
- To check the accuracy level of multiphase flow meter.
- To check the calibration technique of multiphase flow meter.
- Finally, find out the applicability of this process for well testing purpose in other gas fields in Bangladesh.

2.5 Methodology

- Study the metering philosophy of existing multiphase flow meter.
- To collect all relevant data.
- To determine the fluid flow pattern by using Taitel-Dukler Model for Horizontal Flow.
- To find out phase envelope for flow line by using HYSYS Simulator.
- To verify the applicability of working principle on which the flow meter is working for existing flow regime.
- To conduct a thorough investigation for possible causes of metering data inaccuracy.
- To find out alternatives (flow meter) which are compatible for existing fluid pattern.
- Overall adaptability of this flow meter for other gas fields in Bangladesh.

Chapter 3

LITERATURE REVIEW

3.1 Introduction

The need for multiphase flow measurement in the oil and gas production industry has been evident for many years. A number of such meters have been developed since the early eighties by research organizations, meter manufacturers, oil and gas companies and others. Different technologies and various combinations of technologies have been employed and prototype have been quite dissimilar in design and function. Some lines of development have been abandoned, whereas a number of meters are commercially available and the number of applications and users are rapidly increasing.

3.2 Multiphase Flow

Multiphase flow is a complex phenomenon which is difficult to understand, predict and model. Common single phase characteristics such as velocity profile, turbulence and boundary layer, are thus inappropriate for describing the nature of such flows. The flow structures are classified in flow regimes, whose precise characteristics depend on a number of parameters. The distribution of the fluid phases in space and time differs for the various flow regimes and is usually not under the control of the designer or operator [5, 6].

Flow regimes vary depending on operating conditions, fluid properties, flow rates and the orientation and geometry of the pipe through which the fluids flow. The transition between different flow regimes may be a gradual process. The determination of flow regimes in pipes in operation is not easy.

The main mechanism involved in forming the different flow regimes are transient effects, geometry/terrain effects, hydrodynamic effects, and combination of these effects:

- Transients occur as a result of changes in system boundary conditions. This is not to be confused with the local unsteadiness associated with intermittent flow. Opening and closing of valves are examples of operations that cause transient conditions.
- Geometry and terrain effects occur as a result of changes in pipeline geometry or inclination. Such effects can be particularly important in and downstream of sea-lines, and some flow regimes generated in this way can prevail for several kilometers. Severe riser slugging is an example of this effect.
- In the absence of transient and geometry/terrain effects, the steady state flow regime is entirely determined by flow rates, fluid properties, pipe diameter and inclination. Such flow regimes are seen in horizontal straight pipes and are referred to as “hydrodynamic” flow regimes. These are typical flow regimes encountered at a wellhead location.

All flow regimes however, can be grouped into dispersed flow, separated flow, intermittent flow or a combination of these.

- Dispersed flow is characterized by a uniform phase distribution in both the radial and axial directions.
- Separated flow is characterized by a non-continuous phase distribution in the radial direction and a continuous phase distribution in the axial direction.
- Intermittent flow is characterized by being non-continuous in the axial direction and therefore exhibits locally unsteady behavior.

Flow regime effects caused by liquid-liquid interactions are normally significantly less pronounced than those caused by liquid-gas interactions. In this context, the liquid-liquid portion of the flow can therefore often be considered as a dispersed flow. However, some properties of the liquid-liquid mixture depend on the volumetric ratio of the two liquid components.

3.3 Multiphase Flow Regime

Figure 3.1 and Figure 3.3 provide general illustrations of the most flow regimes and indicate where the various flow regimes occur. Physical parameter like density of gas and liquid, viscosity, surface tension, etc. affect the flow regimes and are not included in this graph. A very important factor is the diameter of the flow line, if the liquid and gas flow rates are kept constant and the flow line size is decreased from 4” to 3”, both the superficial gas and liquid velocities will increase by a factor 16/9. Hence, in the two-phase flow map this point will move up and right along the diagonal to a new position. This could cause a change in flow regime, e.g. changing from stratified to slug flow or changing from slug flow to annular flow. Multiphase flow regimes also have no sharp boundaries but instead change smoothly from one regime to another [6].

Most oil wells have multiphase flow in part of their pipe work. Although pressure at the bottom of the well may exceed the bubble point of the oil, the gradual loss of pressure as oil flows from the bottom of the well to the surface leads to an increasing amount of gas escaping from the oil. The diagrams in Figure 3.1 and Figure 3.2 are qualitative illustrations of how flow regime transitions are dependent on superficial gas and liquid velocities in vertical multiphase flow.

The term superficial velocities are often used on the axes of flow regime maps and the definitions are:

- **Superficial Velocities and Mixture Velocity**

  The superficial gas velocity (U_{gs}) is the gas velocity as if the gas was flowing in the pipe without liquids, in other words the total gas throughput (q_g in m^3/s at operating temperature and pressure) divided by the total cross sectional area of the pipe (A). For the superficial liquid velocity the same can be derived, and the simple expressions are given below. They are also referred to as *apparent velocities* or *volumetric fluxes*.

$$U_{ls} = \frac{q_l}{A}\,;\, U_{gs} = \frac{q_g}{A}$$

However, the sum of the superficial velocities are called the mixture velocity,

$$U_{mix} = U_{ls} + U_{gs}$$

3.3.1 Vertical Flows

In vertical flows, the superficial gas velocity will increase in a vertical flow and the multiphase flow will change between all phases, bubble - slug - churn and annular. Note that for a particular superficial gas velocity, the multiphase flow is annular for all superficial liquid velocities.

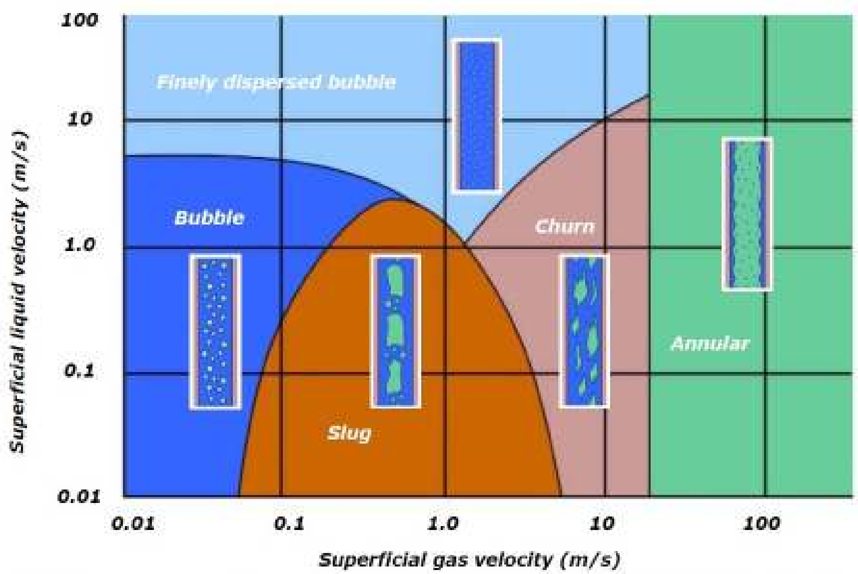

Figure 3.1 Flow Regime Map for Vertical Flow [4]

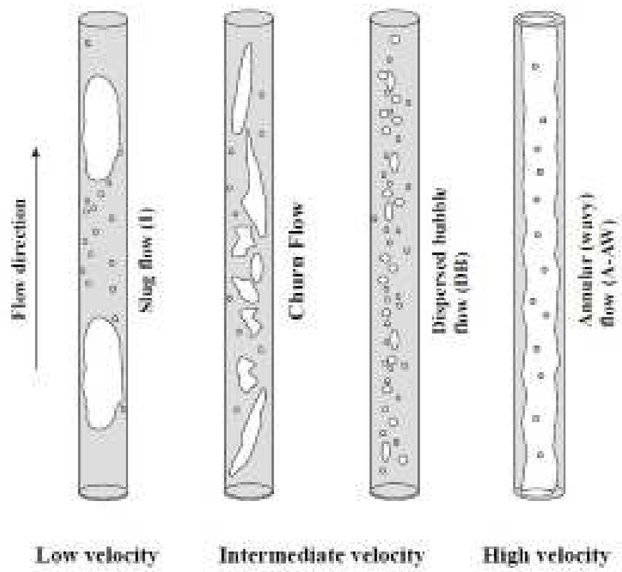

Figure 3.2 Different Types of Flow Profile for Vertical Flow [6]

3.3.2 Horizontal Flows

In horizontal flows too, the transitions are functions of factors such as pipe diameter, interfacial tension and density of the phases. The following map is a qualitative illustration of how flow regime transitions are dependent on superficial gas and liquid velocities in horizontal multiphase flow. A map like this will only be valid for a specific pipe, pressure and a specific multiphase fluid.

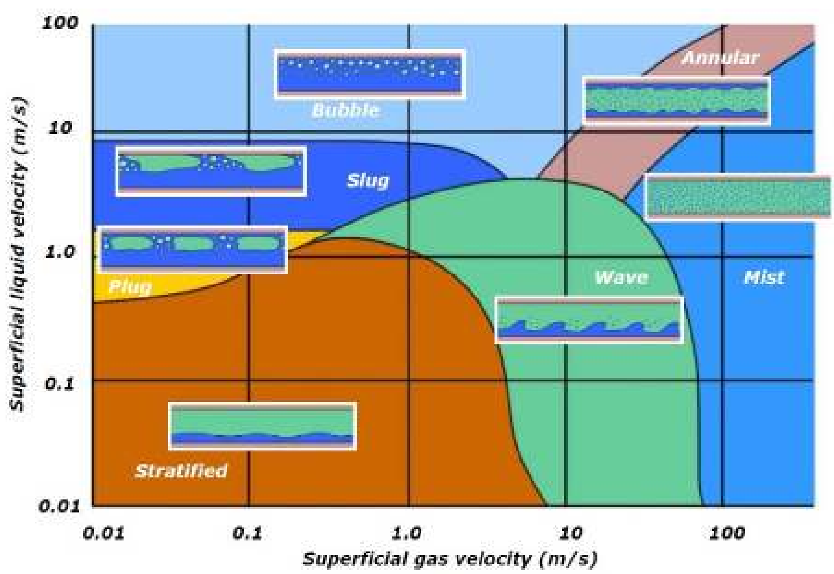

Figure 3.3 Flow Regime Map for Horizontal Flow [4]

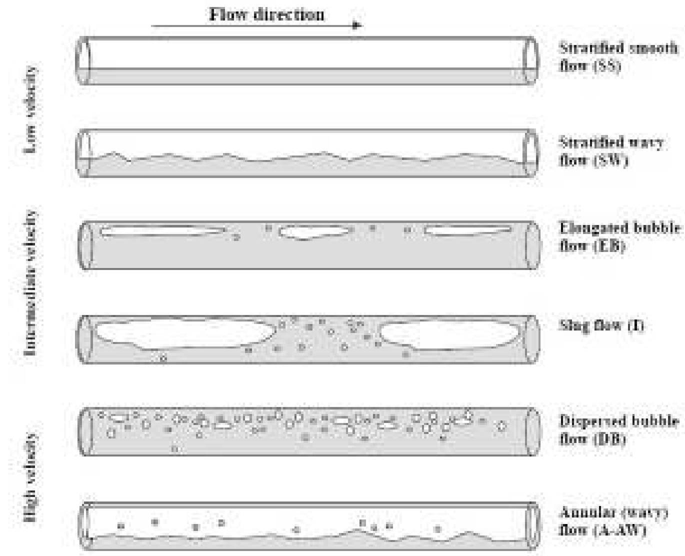

Figure 3.4 Different Types of Flow Profile for Horizontal Flow [6]

Figure 3.2 and Figure 3.4 illustrate the flow regimes in vertical flow and horizontal flow respectively. Figure 3.4 illustrate that at low velocities gas and liquid are separated as in stratified flow. At high velocities gas and liquid become mixed. Slug flow is an example of a flow regime in between, representing both separation and mixing. Slug flow is consequently referred to as an intermittent flow regime. The big difference in between vertical and horizontal flow is that in vertical (concurrent upward) flow it is not possible to obtain stratified flow. The equivalent flow regime at identical flow rates of gas and liquid is slug flow with very slow bullet shaped Taylor bubbles.

3.4 Phase Velocities

The phase velocities are the real velocities of the flowing phases. They may be defined locally (at a certain position in the pipe cross section) or as a cross sectional average for the pipe. They are defined by [6]

$$u_l = \frac{q_l}{A_l};\ u_g = \frac{q_g}{A_g}$$

In order to determine these quantities it is necessary to determine the real flowing cross sections A_l and A_g for liquid and gas. This is equivalent to knowing the fractions or amount of liquid and gas in the flow. From a metering point of view many measurement techniques have been developed to determine the phase velocities.

At first sight it might seem as a trivial matter to measure the phase velocities. In practice however, there is still no "universal" instrument which may function for all flow regimes encountered in two-phase flow.

3.5 Relative Phase Velocities and Slip Effects

Gas and liquid in general flow with different phase velocities in pipe flow. The relative phase velocity or the slip velocity is defined by [6]

$u_l = |u_g - u_l|$

The slip velocity thus has the same unit as the phase velocities. In addition the slip ratio, $S = \frac{u_g}{u_l}$ is commonly used. Note that the slip ratio is dimensionless. It may easily be shown that if the slip ratio is 1 (referred to as no slip) the following relation is valid

$$u_g = u_l = U_{mix}$$

When gas and liquid flow in a pipe, the cross sectional area covered by liquid will be greater than under non-flowing conditions, this is due to the effect of slip between liquid and gas. The lighter gas phase will normally move much faster than the liquid phase; the liquid has the tendency to accumulate in horizontal and inclined pipe segments. The liquid (α_L) or gas fraction (α_G) of the pipe cross sectional area as measured under two-phase flow conditions is known as liquid hold-up (λ_L) and gas void fraction (λ_G). Owing to slip, the liquid hold-up will be larger than the liquid volume fraction. Liquid hold-up is equal to the liquid volume fraction only under conditions of no-slip, when the flow is homogeneous and the two phases travel at equal velocities [5].

$$\text{Liquid hold-up,} \quad \lambda_L = \frac{A_L}{A}$$

$$\text{Gas void fraction,} \quad \lambda_G = \frac{A_G}{A}$$

$$\lambda_L + \lambda_G = 1 \text{ and } \alpha_L + \alpha_G = 1$$

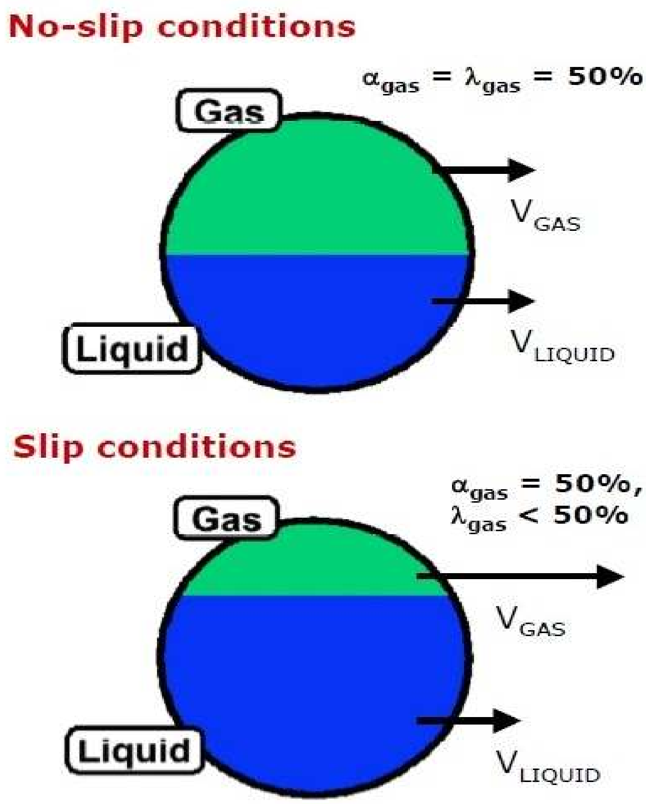

Figure 3.5 Differences between Gas Void Fraction and Gas Volume Fraction [5]

In the majority of flow regimes the Liquid Hold-up will be larger than the Liquid Volume Fraction and the Gas Void Fraction will be smaller than the gas volume fractions which are described in Figure 3.5.

3.6 Fluid Fractions

Gas and fluid fractions are then defined by [6]

$$\varepsilon_g = \frac{V_g}{V} \text{ or } = \frac{A_g}{A} \text{ or } = \frac{L_g}{L} \quad \text{for gas}$$

$$\varepsilon_l = \frac{V_l}{V} \text{ or } = \frac{A_l}{A} \text{ or } = \frac{L_l}{L} \quad \text{for liquid}$$

Where V, A and L are volume, area and length respectively. If the flow pattern was a completely homogenized mixed the three averages would be equal. In two-phase flow terminology ε_g should be referred to as gas fraction; however the term "void fraction" is seen very often. Gas is then considered as absence of liquid (i.e. void). In petroleum industry is still found the symbol H_l instead of ε_l, referred to as liquid holdup [6].

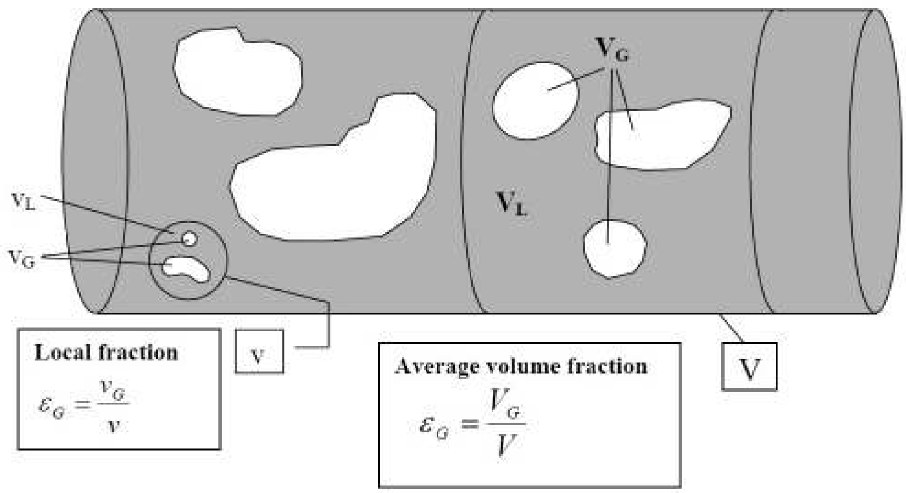

Figure 3.6 Definitions of Volume Fraction [6]

3.7 Mixing Rules

- **Density**
  The density for a two-phase mixture is well defined, geometric quantity that can be calculated provided the fluid fractions are known. The equation is [6]

$$\rho_m = \rho_l \varepsilon_l + \rho_g \varepsilon_g$$

- **Viscosity**
  The mixture viscosity depends on dynamic process as well as including bubble size, flow regime etc. As per Dukler Model the equation is [6]

$$\mu_m = \varepsilon_g \mu_g + (1 - \varepsilon_g)\mu_l$$

3.8 Friction Factor, Shear Stress and Pressure Gradient

The pressure gradient dP/dx in pipe flow depends on pipe diameter D, fluid viscosity μ, fluid density ρ and flow velocity U [6].

In addition the wall roughness and pipe inclination is important. In multiphase flow the flow regime is also important. In single phase and multiphase flow the discrimination between laminar and turbulent flow plays a decisive role for the friction pressure drop. The type of flow is determined from the Reynolds Number

$$Re = \frac{\rho U D}{\mu} \equiv \frac{UD}{\nu} \text{ Where, kinematic viscosity, } \nu = \frac{\mu}{\rho}$$

Classifications of the flow regimes as per Reynolds Number are:

- Re ≤ 2000: Laminar Flow
- 2000 < Re < 4000: Transition between Laminar and Turbulent Flow
- 4000 < Re : Turbulent Flow

Completely turbulent flow is achieved only at very high Reynolds numbers, Re≈ 10^4 - 10^5. The total pressure gradient in the pipe may be considered as composed of 3 different terms:

Frictional pressure gradient, hydrostatic pressure gradient and acceleration pressure gradient. Thus

$$\frac{dp}{dx} = \left(\frac{dp}{dx}\right)_f + \left(\frac{dp}{dx}\right)_h + \left(\frac{dp}{dx}\right)_a$$

- Dimensionless Average Pressure Gradient [7] is defined by

$$\Delta P^* = \frac{\Delta P}{\rho_m g L}$$

Where,
ΔP = Average Pressure Drop
ρ_m = Mixture Density
g = Gravitational Acceleration
L = Length of the Pipe

3.9 Multiphase Composition Map

Composition map is an useful tool in the selection of multiphase flow meters, with sediment and water (S&W) or water cut (WC) in either % or fraction on the x-axis and gas volume fraction in either % or fraction on the y-axis. Although at the outset a producing well would occupy a point on the map, a trajectory for the well can be plotted on the composition map, similar to the well trajectory in the two-phase flow map, as the WC and GVF increase over time. The region that is traversed by the well's trajectory defines its production envelope in the composition map. Similarly, a multiphase flow meter has its characteristic operating envelope in the composition map. Obviously the two envelopes should match if measurement is to be successful [5]. A composition map is shown in Figure 3.7.

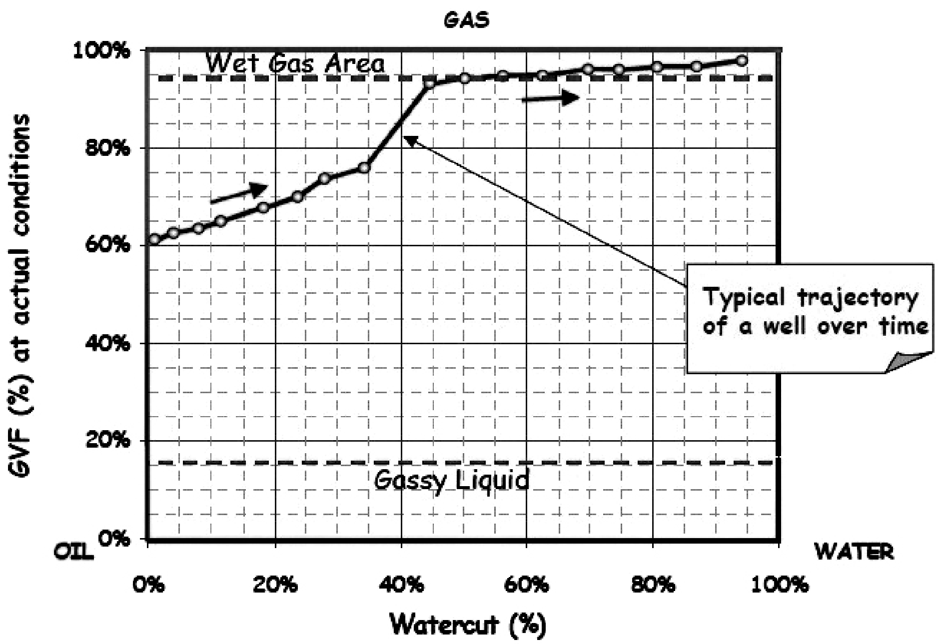

Figure 3.7 Trajectory in Composition Map [5]

3.10 Flow Regime Detection

In transparent pipe it is straightforward to recognize the main types of flow regimes by visual inspection. In offshore pipelines there is little possibility of studying the flow visually. Neither can it be done if the oil is non-transparent or if the flow is so strongly mixed dispersed gas-liquid flow that the mixture becomes non-transparent [6, 7].

3.10.1 Physical Sensor Technique

To determine flow regime automatically, i.e. with an instrument, some kind of "intelligence" must be built into it. This "intelligence" must be capable of finding characteristic features of the flow regime. The most common instruments that are used for flow detection are

- Gamma Ray (or X-Ray) densitometers based on penetration by radioactive beams.
- Impedance (capacitance) sensors based on (oscillating) electric fields.

Pressure and temperature sensor may also be used.

3.10.2 Time Series Analysis

The most common techniques used for analysis of time varying signals work either statistically (probability distribution functions) or by calculating velocities and frequencies.

- **Probability Distributions**

Probability density function is very useful for flow regime determination, because it is quite distinct for most flow regimes. Both average liquid level and amplitude of the fluctuations are important indicators for flow regime determination. We may identify three relatively stationery flow regimes:

- Stratified (wavy) flow
- Dispersed bubble flow
- Annular flow

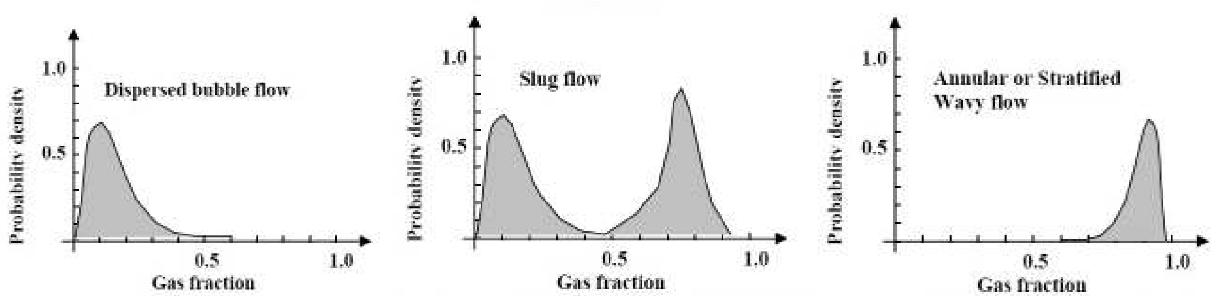

Figure 3.8 Probability Density Functions of various flow regimes [6]

These flow regimes have Probability Density Function's (PDF) with a single peak. Slug flow is fluctuating although it may be considered stationery in contrast to transient.

This means that the liquid level will fluctuate all the time, but on a long term a stationery PDF will build up. This PDF is a bimodal type with two peaks, a very distinct characteristic of slug flow. Typical PDF's for the various regimes are shown in the Figure 3.8. The PDF of *Annular* flow and *Stratified Wavy* flow may look quite similar. Also *Dispersed Bubble* flow and *Stratified Wavy* flow with high liquid level may be difficult to distinguish. In such cases it may be necessary to use supplementary analysis in which also flow dynamics can be determined.

- **Frequency Spectrum Analysis**

The frequency spectrum is obtained from a time series f(t) by using the Fourier transform F(ω). It is calculated as

$$F(\omega) = \int_{-\infty}^{\infty} f(t) \exp(-i\omega t) dt$$

Where "i" is the imaginary number unit and ω is the oscillation angular velocity, which is related to frequency by $\omega = 2\pi f$.

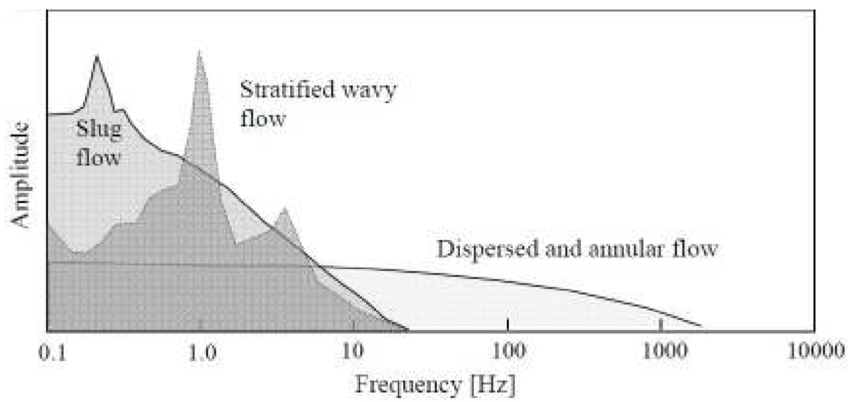

Figure 3.9 Frequency spectra of gas fraction in various flow regimes [6]

The frequency spectrum is often defined by the square module of F(ω) in order to become real. A simple sine wave has only one frequency and the spectrum will have only one peak, as shown in Figure 3.9. In comparison, a strongly fluctuating signal will be characterized by a broad spectrum where a range of frequencies appear.

3.10.3 Tomography

It is in principle possible to determine the distribution of gas and liquid in the pipe cross section by using a set of sensors with individual different spatial sensitivity. This enables tomographic analysis of the flow. Well known physical principles are X-Ray and Gamma-Ray based tomography often referred to as CT (Computed Tomography) as well as Nuclear Magnetic Resonance (NMR). Tomography is mainly used for medical imaging but has also been used for multiphase flow. However the tomography technique require a scan time of typically seconds for a single spatial scan and is very expensive. X-Ray techniques in comparison are very fast and typically giving up to 1000 frames/second. Also impedance techniques are very fast. They are also very inexpensive and imply no health hazards [7].

3.11 Phenomenological Flow Regime Model

Horizontal and vertical flows represent extremes concerning geometrical conditions for flow regimes, of course due to the impact of gravitational forces. The term "physical model" is sometimes used to describe a *laboratory flow loop* as opposed to a full scale flow loop, as opposed to a mathematical model which is a set of equations.

3.11.1 Horizontal Flow - The Taitel and Dukler Model

The model published by Taitel and Dukler in 1976, has become a classic example of how to combine experiment and theory into a model without having to be completely empirical, i.e. without having to use correlations of pure curve fit type. It may be criticized for simplification and choice of specific assumptions, however it will be standing as a method to develop useful calculation tools with a deeper understanding. The flow regimes arise a competition between the most important forces that act-gravitation (with buoyancy), turbulence, interfacial friction and lift forces (Bernoulli Effect). To calculate the three latter forces one needs the phase velocity of gas and liquid. If only the superficial velocities are known, it is necessary to calculate the fluid fraction before one can find the phase velocities [6, 8, 9].

Flow Model Assumptions:

- Stratified without waves
- Constant gas density
- Isothermal flow (no thermal effects on density and viscosity)
- Steady state flow

Liquid Fraction in horizontal stratified flow:

Consider a near horizontal flow as shown in the Figure 3.10, with above assumptions and further assumed that forces are in equilibrium and equations are [6]:

Liquid: $-A_L\left(\frac{dP}{dx}\right)_L - \tau_L S_L + \tau_i S_i + \rho_L A_L \, \mathrm{g} \sin\beta = 0$

Gas: $-A_G\left(\frac{dP}{dx}\right)_G - \tau_G S_G - \tau_i S_i + \rho_G A_G \, \mathrm{g} \sin\beta = 0$

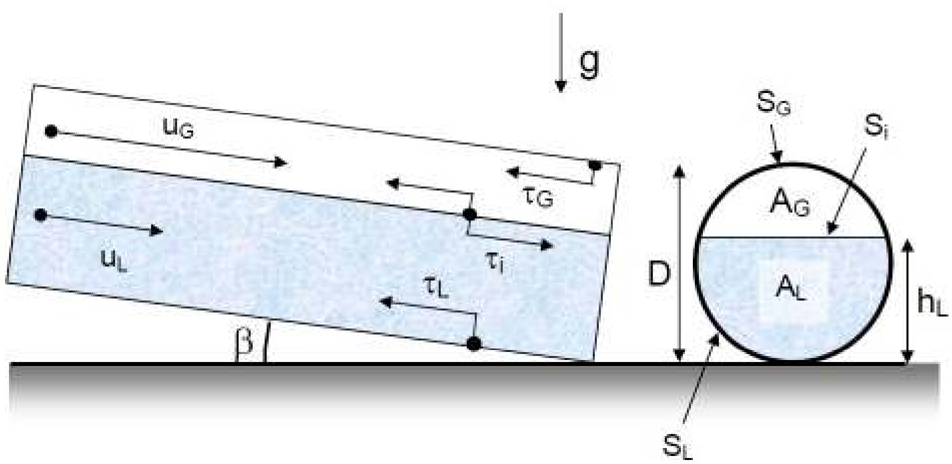

Figure 3.10 Taitel and Dukler Model for Stratified near horizontal flow [6]

These equation may be considered as space and time averaged versions of the Navier-Stokes equations for two phase flow. Provided the liquid height remains constant along the flow, we may use the relation $\left(\frac{dP}{dx}\right)_L = \left(\frac{dP}{dx}\right)_G = \left(\frac{dP}{dx}\right)$, and eliminate the pressure gradient from the two equations and obtain [6]

$$\tau_G \frac{S_G}{A_G} - \tau_L \frac{S_L}{A_L} + \tau_i S_i \left(\frac{1}{A_L} + \frac{1}{A_G}\right) + (\rho_L - \rho_G)\, \mathrm{g} \sin\beta = 0$$

In this equation the shear stresses are modeled as:

$$\tau_L = f_L \frac{\rho_L U_L^2}{2}$$

$$\tau_G = f_G \frac{\rho_G U_G^2}{2}$$

$$\tau_i = f_i \frac{\rho_G (U_G - U_L)^2}{2}$$

The friction factors enter the shear stress equations as in single flow. However, the geometry of the fluid wall contact no longer circular and the following expressions are used.

$$f_L = C_L \left(\frac{D_L U_L}{\vartheta_L}\right)^{-n}$$

$$f_G = C_G \left(\frac{D_G U_G}{\vartheta_G}\right)^{-m}$$

$$f_i \approx f_G$$

The pipe diameter D is replaced by the equivalent hydraulic diameter D_L and D_G. These are defined as in

For Liquid (Open Channel) $D_L = \frac{4A_L}{S_L}$

For Gas (closed duct) $D_G = \frac{4A_G}{S_G + S_i}$

The assumption that the friction factor $f_i \approx f_G$ is based on experiments with stratified flow without waves. The procedure now is to transform the previous equations into a form where the superficial velocities appear instead of the phase velocities and where the liquid fraction (liquid height) appears in separate terms. To do this we need to introduce dimensionless quantities by scaling the corresponding dimensional quantities in the following way: all lengths are divided by D, areas are divided by D^2 and phase velocities are divide by their corresponding superficial velocities. We also introduce $\widetilde{h_L} = \frac{h_L}{D}$ and obtain [6]

$$\tilde{S}_G = \frac{S_G}{D} = arccos\left(2\tilde{h}_L - 1\right)\tilde{S}_L = \frac{S_L}{D} = \pi - \tilde{S}_G\tilde{S}_i = \frac{S_i}{D} = \sqrt{1 - \left(2\tilde{h}_L - 1\right)^2}$$

$$\widetilde{D}_L = \frac{D_L}{D} = \frac{4\tilde{A}_L}{S_L}\widetilde{D}_G = \frac{D_G}{D} = \frac{4\tilde{A}_G}{S_G + S_i}\tilde{A} = \frac{\pi}{4}$$

$$\tilde{A}_G = \frac{A_G}{D^2} = \frac{1}{4}\left[arccos\left(2\tilde{h}_L - 1\right) - \left(2\tilde{h}_L - 1\right)\sqrt{1 - \left(2\tilde{h}_L - 1\right)^2}\right]$$

$$\tilde{A}_L = \frac{A_G}{D^2} = \frac{\pi}{4} - \tilde{A}_G\widetilde{U}_L = \frac{U_L}{U_{LS}} = \frac{\tilde{A}}{\tilde{A}_L}\widetilde{U}_G = \frac{U_G}{U_{GS}} = \frac{\tilde{A}}{\tilde{A}_G}$$

Dimensionless combined momentum equations [6]:

$$X^2\left[\left(\widetilde{U}_L\widetilde{D}_L\right)^{-n}\widetilde{U}_L^2\frac{\tilde{S}_L}{\tilde{A}_L}\right] - \left[\left(\widetilde{U}_G\widetilde{D}_G\right)^{-m}\widetilde{U}_G^2\left(\frac{\tilde{S}_G}{\tilde{A}_G} + \frac{\tilde{S}_i}{\tilde{A}_L} + \frac{\tilde{S}_i}{\tilde{A}_G}\right)\right] - 4Y = 0$$

Where, $X^2 = \left|\frac{\left(\frac{dP}{dx}\right)_{LS}}{\left(\frac{dP}{dx}\right)_{GS}}\right|$ and $Y = \frac{(\rho_L - \rho_G)\,g\sin\beta}{\left(\frac{dP}{dx}\right)_{GS}}$

The superficial pressure drops $\left(\frac{dP}{dx}\right)_{GS}$ and $\left(\frac{dP}{dx}\right)_{LS}$ are calculated as for single phase flow, based on gas and liquid superficial velocities and the respective single phase fluid properties.

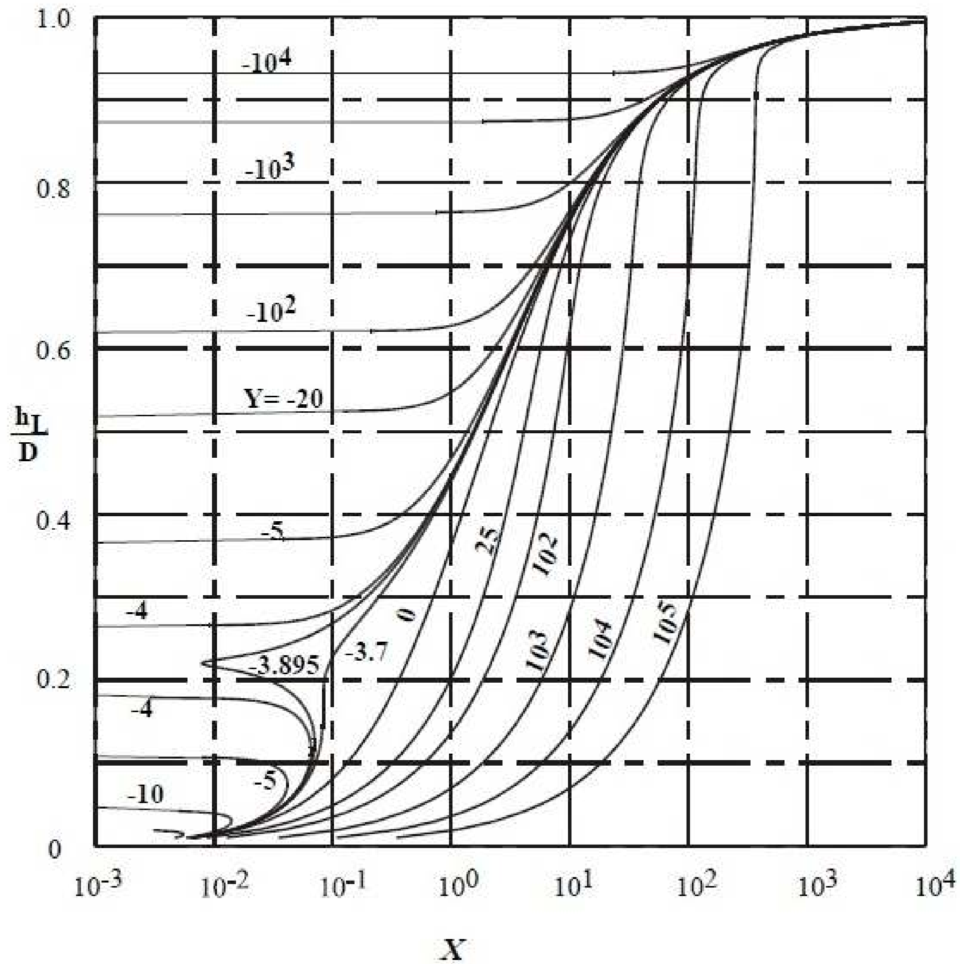

Figure 3.11 Equilibrium liquid levelas a function of the Lockhart-Martinelli parameter [6]

In the Figure 3.11 is shown the solution of the dimensionless liquid fraction equation for different values of Y with the Lockhart-Martinelli parameter X as abscissa. The equation is transcendent in $\tilde{h}_L$ is to be found as a function of X.

3.12 Models for Flow Regime Transition

Starting from the superficial velocities and liquid fraction the real velocities (phase velocities) can be calculated. These now enter models for flow regime borders [6, 9]. We discuss the four borders which are essential, describing the transition between:

3.12.1 Stratified flow with and without waves
3.12.2 Stratified flow and slug flow

3.12.3 Slug flow and dispersed bubble flow
3.12.4 Slug flow and annular flow

3.12.1 Transition between stratified flow with and without waves

On a plane liquid surface waves can be generated in various ways. We are primarily interested in waves arising from gas blowing over the surface. Taitel and Dukler adopt a model by Jeffreys (1926) who suggested the following condition for wave generation [6, 9, 10].

$$C.(U_G - C)^2 \geq \frac{4\vartheta_L g(\rho_l - \rho_g)}{s\rho_g}$$

Here C is the wave velocity and s is a “screening coefficient” which in value is 0.3 according to Jeffreys. In the model by Taitel and Dukler the value S= 0.01 is used. At increasing Reynolds number the ratio $\frac{C}{U_L}$approaches unity and for simplicity we may assume $C = U_L$. We further assume that $U_G \gg C$ and thus obtain the criterion for wave generation as

$$U_G \geq \left[\frac{4\vartheta_L(\rho_L - \rho_G)gcos\beta}{S\rho_G U_L}\right]^{\frac{1}{2}}$$

The pipe inclination β has been included to make it possible to apply the expression also for slightly inclined pipes. In this case we use an effective gravity constant $gcos\beta$.

3.12.2 Transition between stratified flow and slug flow

The instability where stratified flow transforms to slug flow is called the *Kelvin-Helmholtz instability* which describes in Figure 3.12. When the gas velocity becomes sufficiently high, waves become unstable due to Bernoulli lift effects. The reduced gas flow area over the wave top leads to pressure drop which lifts the waves. If the lift is stronger than a critical value given by the wave mass, the waves will be lifted to entirely the whole pipe cross section. This process is spontaneous and very fast, provided the conditions are present. We will develop a simple which yields the proper equation for the transition. The quantities that are used to describe the instability is U_G and the characteristic heights h_G and h_L [6, 9, 10].

The original analysis was carried out for flow between two infinite planes, by means of wave theory, which is too comprehensive to be done here. They obtained the classical criterion

$$U_G > \left[\frac{g(\rho_L - \rho_G)h_G}{\rho_G}\right]^{\frac{1}{2}}$$

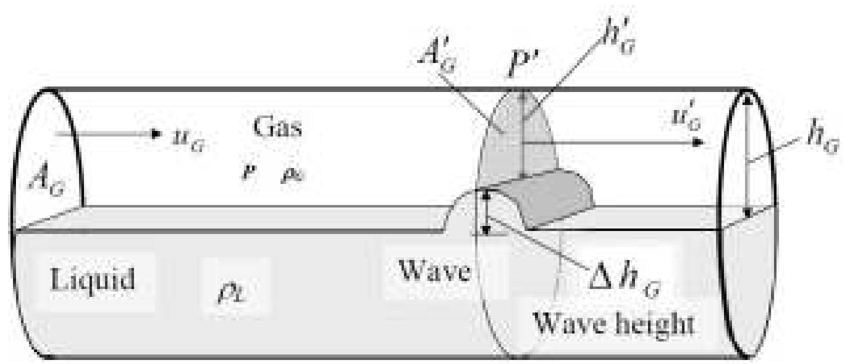

Figure 3.12 Wave generation leading to the Kelvin-Helmholtz instability [6]

We instead use Bernoulli's equation and assume that ρ_G is constant along the interval. For circular pipes the gas flow area is not linearly dependent on h_G and the solution is more complex. By straightforward manipulation of the previous conditions we get [6]

$$U_G > \left[\frac{2(\rho_L - \rho_G)g cos\beta\left(\acute{h}_L - h_L\right)}{\rho_G} . \frac{\acute{A}_G^2}{A_G^2 - \acute{A}_G^2}\right]^{\frac{1}{2}}$$

For small waves $\acute{A}_G$ can be Taylor expanded to give the final expression

$$U_G > C_2 \left[\frac{(\rho_L - \rho_G) g cos\beta A_G}{\rho_G S_i}\right]^{\frac{1}{2}}$$

Where we have used $S_i = \frac{d\tilde{A}_L}{d\tilde{h}_L}$ with $C_2 = \left[2\frac{(\acute{A}_G/A_G)}{1+\acute{A}_G/A_G}\right]^{\frac{1}{2}}$

The function C_2 is wave height dependent, in general unknown and non-linear. However, simple inspection shows that it has the following limits:

- For low liquid height (and small disturbances) $\acute{A}_G \to A_G$. Thus C_2 approaches 1.0.
- For high liquid level $\acute{A}_G$ is very sensitive to even small waves and approaches zero. In this case also C_2 approaches zero.

A simple function for this behavior is the linear, $C_2 = 1 - \frac{h_L}{D} = 1 - \tilde{h}_L$.

3.12.3 Transition between slug flow and dispersed bubble flow

If the liquid flow rate is large (absolute and in comparison to the gas flow rate), the liquid fraction will be high and also the flow velocity. The degree of turbulent mixing then also is important and eventual gas will be broken into small dispersed bubbles. In the Taitel and Dukler theory a transition criterion has been introduced based on balance between buoyancy and turbulence. Buoyancy causes the gas bubbles to migrate towards the upper part of the pipe and coalesce to form large gas bubbles and slug flow. Turbulence on the other hand mainly breaks bubbles apart and diffuses the bubbles over the pipe cross section, thus favoring dispersed bubble flow. Figure 3.13 for the discussion to follow. Imagine the flow is at the transition between slug flow and dispersed bubble flow. The large gas bubble is exposed to the high velocity turbulent liquid flow on the bottom interface side and front and rear sides. On the other hand the buoyancy acts upwards to recover the large bubble [5, 7, 10].

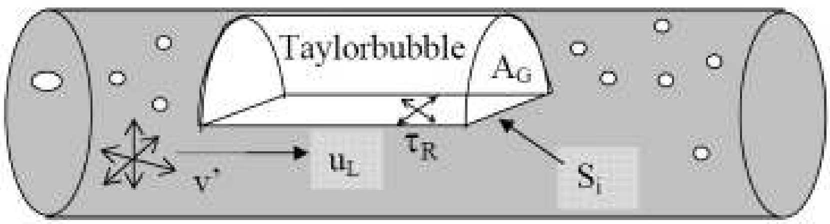

Figure 3.13 Taylor bubble on the transition to dispersed bubble flow [6]

3.12.4 Transition between slug flow and annular flow

If the gas velocity is sufficiently high to exceed stratified flow, e.g. by the Kelvin-Helmholtz criterion, there is still a possibility that slug flow does not occur. This is the case if the gas flow rate is so high that gas blows through and destabilizes the slugs. In this case annular type flow occurs. Taitel and Dukler present a highly simplified argument to quantify this phenomenon. They assume that equilibrium level is the most important contribution. The mechanism is illustrated in the figure below. In order to maintain slug there at least must be sufficient liquid to create the slug.

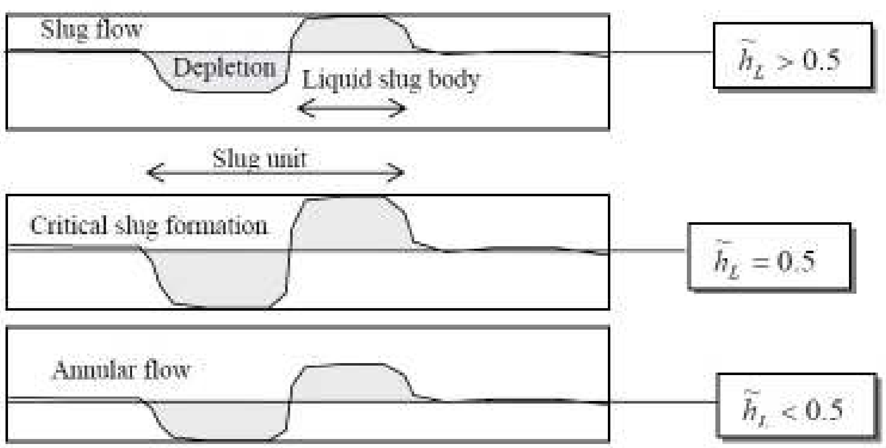

Figure 3.14 Slug-Annular Flow Transition [6]

Figure 3.14 illustrates slug-annular flow transition. If the average liquid level drops below 50% there will not be sufficient liquid to develop a stable slug. The amount of liquid in the slug body equals the amount of liquid removed from the neighboring depletion.

The slug creation takes place in very short time and the required liquid must be taken from the immediate surroundings. In the critical case with 50% liquid ($\tilde{h}_L = 0.5$) the slug needs all surrounding liquid. If the liquid level is less than 50% this is still not sufficient to establish full liquid slug; gas blows over the liquid and annular flow results. A modified criterion has later been suggested by Taitel and Dukler. It is observed in high velocity slug flow that the liquid slug body may contain up to 30% gas. In the critical case the average liquid fraction over the slug unit (liquid slug body and neighboring depletion) is

$$\varepsilon_L = \frac{1}{2}(0 + 0.7) = 0.35$$

A logical flow diagram of Taitel-Dukler Model is presented in figure 3.15 on the next page.

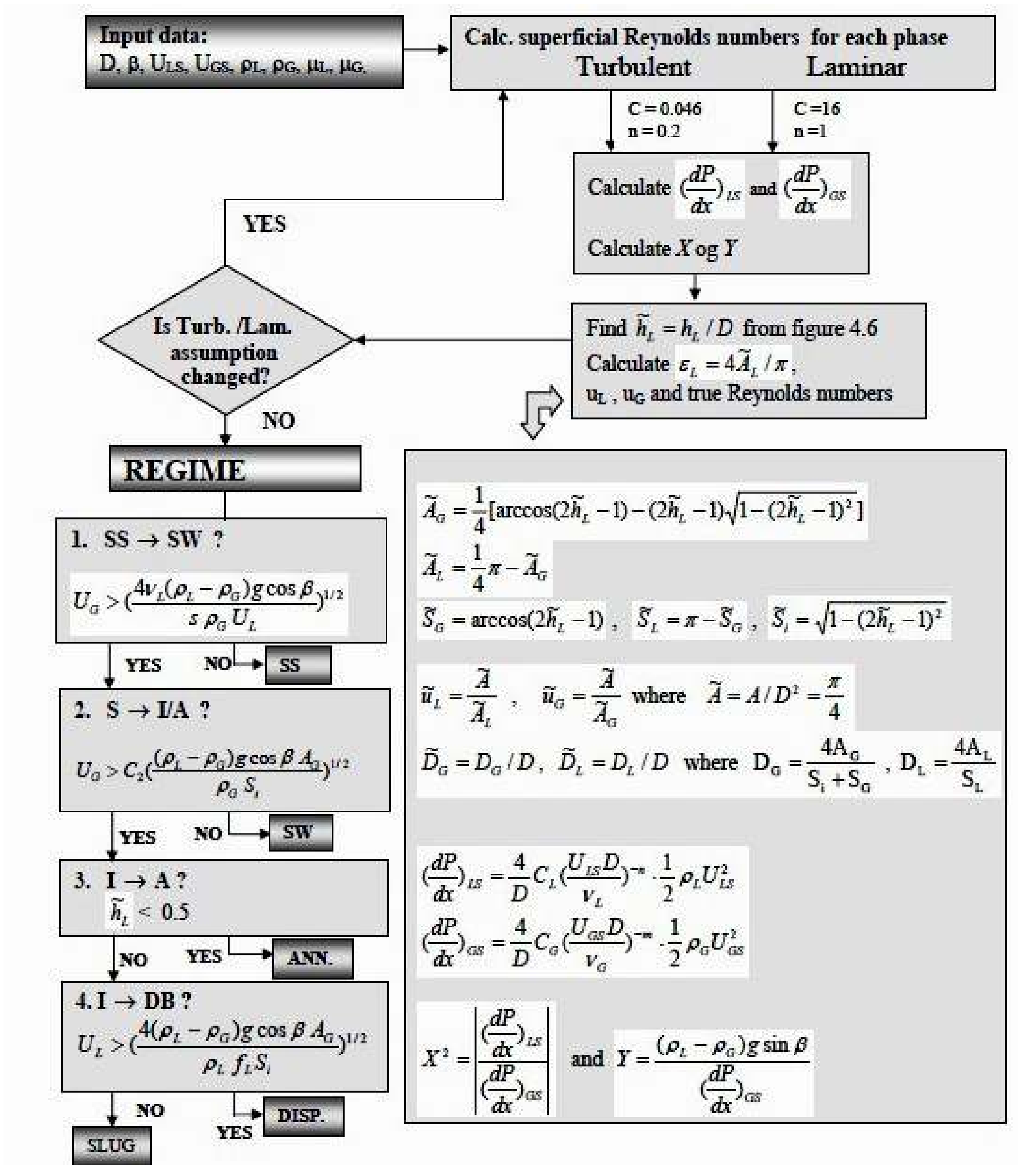

Figure 3.15 Taitel and Dukler Model-Logical Flow Diagram [6]

3.13 The Lockhart-Martinelli Correlation

The Lockhart-Martinelli correlation was originally developed for calculation of pipe flow pressure drop in nuclear plant cooling systems. Later it has been adopted also for petroleum applications. The model is very simple and can be characterized as a separated flow model. This means that it considers the total frictional pressure gradient as composed of separate liquid and a gas terms based on the superficial pressure drops. A simple interaction term is used to describe interfacial shear forces. This does not mean that the model is applicable only to separated (e.g. stratified flow) [6, 9, 10]

However, conceptually one may visualize the model as if the total flow in one single pipe with diameter D was split into two identical pipes with identical diameters as the original (D), each pipe transporting only gas or only liquid. The pressure drop in each pipe would then equal the superficial pressure drop.

However, in the real process the phases interact. This interaction is then modeled as if there was some link between the pipes, so that one might express the interaction by some function of the individual pressure drops. The interaction term suggested by Lockhart and Martinelli was a geometrical mean of the individual pressure drops.

$$\left(\frac{dP}{dx}\right)_f = \left(\frac{dP}{dx}\right)_{GS} + C.\sqrt{\left(\frac{dP}{dx}\right)_{GS}.\left(\frac{dP}{dx}\right)_{LS}} + \left(\frac{dP}{dx}\right)_{LS}$$

The "coupling constant" C depends on the single phase flow regimes (laminar or turbulent) given by the Reynolds numbers. The appropriate C values are given in the Table 3.1. Note that C approximately doubles each time one of the phases goes from laminar to turbulent.

Table 3.1 "C" Values for the Lockhart-Martinelli Model [6]

Liquid Regime	Gas Regime	Subscript	C
Turbulent	Turbulent	tt	20
Viscous (lam.)	Turbulent	vt	12
Turbulent	Viscous (lam.)	tv	10
Viscous (lam.)	Viscous (lam.)	vv	5

Depending on the choice we get the two following expressions [6]:

$$\left(\frac{dP}{dx}\right)_f = [1 + C.X + X^2].\left(\frac{dP}{dx}\right)_{GS} \equiv \varphi_G^2.\left(\frac{dP}{dx}\right)_{GS}$$

$$\left(\frac{dP}{dx}\right)_f = \left[1 + C.\frac{1}{X} + \frac{1}{X^2}\right].\left(\frac{dP}{dx}\right)_{LS} \equiv \varphi_L^2.\left(\frac{dP}{dx}\right)_{LS}$$

Where the Lockhart-Martinelli parameter is given by $X^2 = \frac{\left(\frac{dP}{dx}\right)_{LS}}{\left(\frac{dP}{dx}\right)_{GS}}$

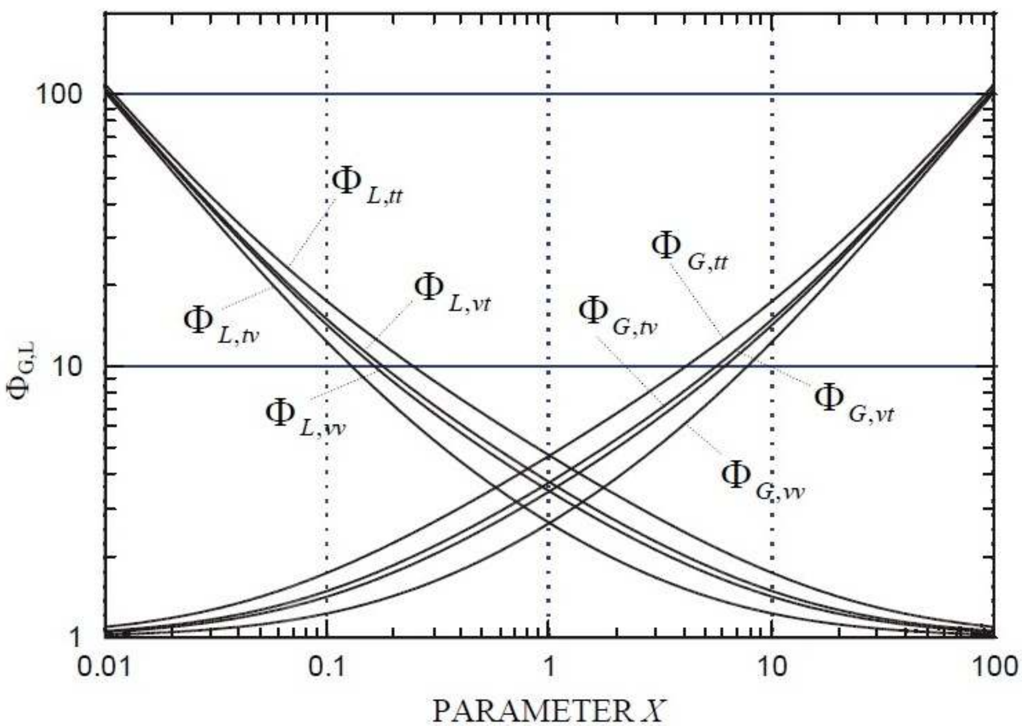

Figure 3.16 Two-phase multiplier φ in the Lockhart-Martinelli Correlation [6]

On the other hand the two-phase multipliers φ_G^2 and φ_L^2 can be considered as function of *X*. In this case the "flow regime" is allocated entirely to the coefficient C. It is the various values of C that identify the various curves in Figure 3.16.

3.14 Measurement Techniques

There is a variety of techniques that have been investigated for this application during last 20-30 years. Multiphase flow is industrial technology, as well as a science and consequently the usefulness of various techniques varies from one application to the other. There is a large span in instrument parameters like size, complexity, price and even hazards involved by use from one technique to the other. The most common techniques from the petroleum production point of view, which concern measurement of:

- Fluid fractions
- Flow regimes
- Phase flow velocities and flow rates

3.14.1 Measurement of fluid fractions by gamma densitometer

The gamma (γ) densitometer consists in principle of a radioactive source which irradiates the pipe flow line with penetrating gamma rays. A detector on the opposite side registers the particles that pas through the pipe walls and the two-phase flow mixture [11]. Figure 3.17 describes the principle of Gamma Densitometer.

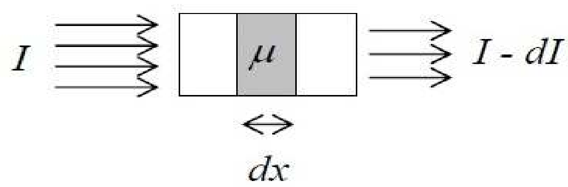

Figure 3.17 Principle of Gamma Densitometer [11]

The absorption of gamma particles obey the differential equation:

$$dI = -\mu . I . dx$$

Where, *dI* is the of radiation through a length *dx* of the medium that the beam penetrates. The attenuation constant is material dependent and is to a large extent proportional to the density of the medium. The differential equation is solved straightforward to yields *Beers Attenuation Law:*

$$I(x) = I_0 . e^{-\mu x}$$

Where, *I(x)* is the remaining beam intensity after having traversed a length x of the medium starting with intensity I_0 at the entrance $x = 0$. The gamma ray energy from 50 keV to 1 MeV.

Gamma rays are produced by radioactive sources of various radioactive isotopes. Also X-rays may be used, which are produced by X-ray generators. However X-rays are normally low energetic, ranging from a few keV to 200 keV. For a homogeneous mixture the attenuation constant can be written as

$$\mu = \left(\frac{N_0}{A}\right) \sigma \rho_m$$

Where N_0 is Avogadro number, A is the atomic mass number, σ is the atomic absorption cross section (in cm^2/g) and ρ_m is the mixture density. The atomic cross section varies with the gamma energy and the material irradiated.

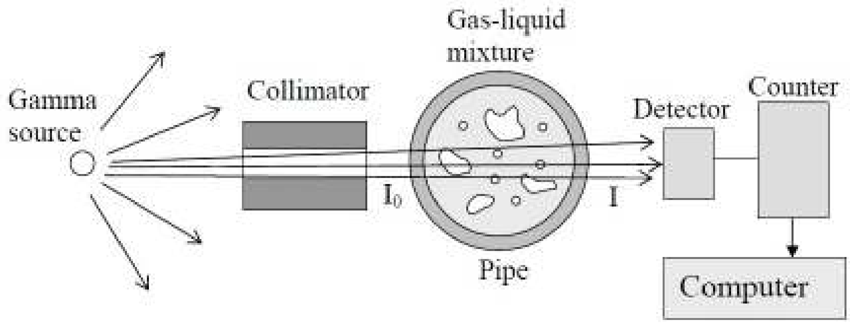

Figure 3.18 Principle design of Gamma Densitometer [11]

If the gas liquid flow regime is dispersed (homogeneous) as per Figure 3.18 it can be derive the following relation for measurement of gas fraction:

$$\varepsilon_G = \frac{\ln(I/I_L)}{\ln(I_G/I_L)}$$

Where I is measured intensity reaching the detector when having two-phase flow. On the other hand I_G and I_L are the measured intensities if either only gas or only liquid is present in the pipe. Normally $I_G \gg I_L$. For other flow regimes where the gas and liquid come as consecutive sections along the beam path the same equation as above applies. However, for flow regimes where gas and liquid are parallel along the beam direction the appropriate equation is

$$\varepsilon_G = \frac{I - I_L}{I_G - I_L}$$

3.14.2 The Venturi flowmetere

It is based on the pressure drop associated with increase of flow speed as predicted by the Bernoulli equation [7].

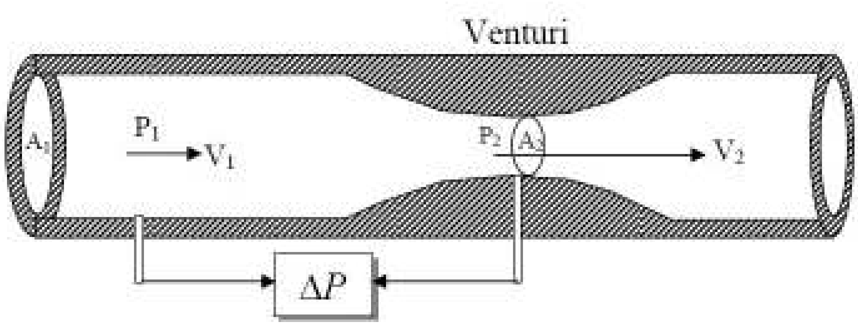

Figure 3.19 Venturi Flowmeter Principle [11]

With reference to the Figure 3.19 the equation may write as

$$P_1 + \frac{1}{2}\rho_1 V_1^2 = P_2 + \frac{1}{2}\rho_2 V_2^2$$

If hydrostatic pressure gradient and friction may be neglected. If the density may be assumed constant, the continuity equation may be written

$$V_1 . A_1 = V_2 . A_2$$

And we obtain the volumetric flow rate $Q = V_2 . A_2$ as $Q = \frac{A_2}{\sqrt{1-\beta^2}}\sqrt{\frac{2.\Delta P}{\rho}}$

The equivalent mass flow rate $G = \rho . Q$ is then $G = \frac{A_2}{\sqrt{1-\beta^2}}\sqrt{2.\rho.\Delta P}$

Where $\beta = \frac{A_2}{A_1}$ and the pressure drop $\Delta P = P_1 - P_2$. In practical application there are always some extra pressure losses which must be compensated. These may be put into a discharge coefficient C_d which account for additional flow effects. Thus

$$G = \frac{C_d A_2}{\sqrt{1-\beta^2}}\sqrt{2.\rho.\Delta P}$$

3.14.3 Wet Gas Meter

The Wet Gas Meter (WGM) detects the water content based on microwave technology and flow rates using a V-cone differential pressure device. The split between gas and condensate is found using PVT Calculations and as such, the meter depends on input of the true hydrocarbon composition. Figure 3.20 is a schematic diagram of wet gas meter arrangement.

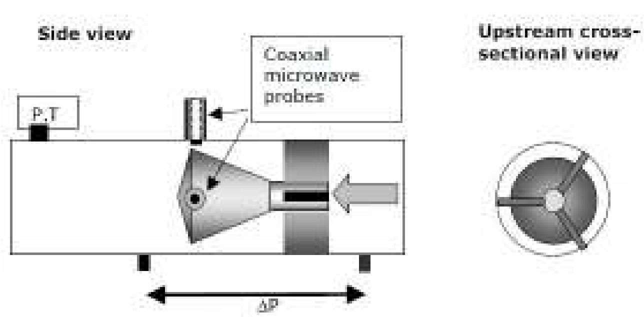

Figure 3.20 V-Cone Wet Gas Meter Principle [3]

3.14.3.1 V-Cone Differential Pressure Flow meter

The individual flow rates are measured using a V-Cone differential pressure flow meter. The measured differential pressure basically depends on fluid density, composition and flow velocity [4, 11, 12]. In the case of two phase wet gas flow, the gas rate is generally expressed as:

$$Q_g = \frac{\pi D^2}{4}\frac{C_D . y}{\emptyset_G}\sqrt{\frac{2. \Delta p. \rho g}{(\beta^{-4} - 1)}}$$

Where, C_D = Gas discharge

y = Fluid expansibility

$\emptyset_G$ = Two phase gas multiplier

The WGM can be equipped with dual set of differential pressure transmitter for redundant measurements.

3.14.3.2 Microwave based Water Fraction Meter

The Water Fraction Meter (WFM) detects the resonant frequency of microwave radiation propagating through a fluid mixture that is instantaneously present in the resonance cavity. The resonant frequency depends on the dielectric properties of the mixture, which is a function of fluid fractions, temperature and water conductivity [11, 12, 13].

The permittivity of water (~60-200) is much higher than that of gas (~1) or oil/condensate (~2). The dielectric properties of the wet gas mixture are consequently very sensitive to the water content and the WFM is basically used to deduce the water volume fraction α_w.

The resonant frequency is generally given by [11]:

$$f_r = f_{vac}/\sqrt{\varepsilon_{mix}}$$

Where,

f_{vac} = Vacuum Frequency

ε_{mix} = Mixture Permittivity

and this resonant frequency can be calculated from the permittivity of each of the constituting materials (water, gas, condensate) and the individual volume fractions through using certain mixing formulas. All Multiphase flow meters are based on the *Brǜggeman mixing formula* [11]:

$$1\text{-}\alpha_i = \frac{\varepsilon_i - \varepsilon_{mix}}{\varepsilon_i - \varepsilon_h} . (\varepsilon_h/\varepsilon_{mix})^{1/3}$$

Where,

ε_{mix} = Mixture Permittivity;

ε_h = Permittivity of the continuous host material (gas);

ε_i = Permittivity of the inclusion material (condensate or water);

α_i = Volume fraction of the inclusion material

The measured water fraction is compensated for the presence of water vapor and the appearance of slip in the WFM sensor.

3.14.3.3 Microwave based Formation Water Detection

A microwave resonator sensor has a resonance that is used for measurement purposes. The resonance has mainly two properties: The resonance frequency f_r and the quality factor Q. The quality factor is defined as the ratio between resonant frequency and the half-power width of the resonance peak [11, 12, 13]:

$$Q = \frac{f_r}{\Delta f_{hp}}$$

Both f_r and Q are affected by the permittivity of the mixture being measured. The permittivity is a complex quantity, i.e. it has both a real and an imaginary part, which means that it is actually a combination of two more or less independent quantities [11]:

$$\varepsilon_r = \varepsilon_r' - j\varepsilon_r''$$

The subscript r means that the permittivity is taken relative to that of vacuum. Physically the real part gives the speed of propagation, i.e. tells how much the waves are being slowed down by the medium. The slowing of the waves also means that the wavelength is shorter in the medium than in vacuum. Therefore the phase shift experienced on a fixed distance is larger in the medium. Because the resonance condition of a microwave resonator is fulfilled at a fixed wavelength, the resonant frequency decreases with increasing permittivity according to

$$f_r = \frac{f_{ro}}{\sqrt{\varepsilon'_r}}$$

Where, f_{ro} = resonant frequency of the empty sensor

The imaginary part tells how fast a propagating wave is attenuated, i.e. how lossy the medium is. The losses broaden the resonance peak. When the losses in the medium is the main loss mechanism in the resonator, the quality factor is

$$Q \approx \frac{\varepsilon''_r}{\varepsilon'_r}$$

Ionic conductivity is associated with resistive losses. The conductivity σ in the medium gives rise to a component of the imaginary part of the permittivity:

$$\varepsilon''_{r\sigma} = \frac{\sigma}{2\pi f \varepsilon_o}$$

Where, $\varepsilon_o = 8.854\text{x}10^{-12}$ As/Vm is the permittivity of vacuuam.

The permittivity of the mixture depends on the permittivity of the constituents. This is the basis for all microwave composition measurements. If the water droplets of an oil or gas continuous mixture are conductive, the whole mixture is lossy. By measuring both f_r and Q, both the WVF and the lossiness of mixture increases and is detected as a reduction in Q. Figure 3.21 shows how electromagnetic field of V-Cone Resonator are distributed.

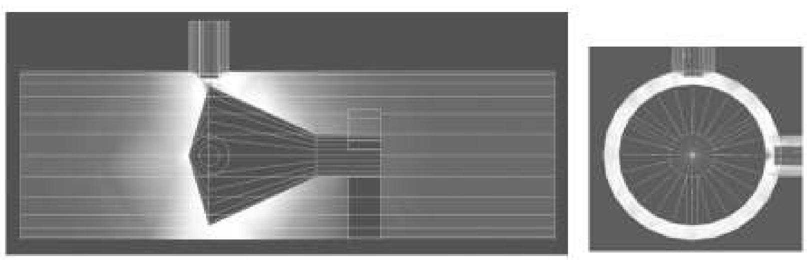

Figure 3.21 Electromagnetic Field Distribution of V-Cone Resonator [11]

3.15 Factors influence the measurement of Multiphase Flow Meter

PVT data of fluid stream affects in the performance of Multiphase Flow Meter. For high GVF (~98%) the gas phase is very little affected by PVT errors and with rapidly changing composition has significant impact on MFM data. Beside PVT data, some other factors listed in the Table 3.2 can contribute for biasing meter data [5, 7, 14].

Table 3.2 List of Influencing Factors for MFM Bias Result [5]

Nature of Influence	Specific Influence	Effect on Measurement
Sensor Drift	Drift of DP, P, T	Bias calculation of flow rate, conversion to standard condition etc.
	Count rate drift	Cause bias in density or phase fraction
	Radiation Detector Resolution	Causes errors in phase fractions for dual-energy gamma-ray instruments
Operating Environment	Pressure	Operating limits, transducer damage, offset due to static pressure
	Temperature	Operating limits, transducer damage, offset to low or elevated temperature
	Slip Ratio	Wrong correction made for slip between gas and liquid
	Flow Regime/Pipe Orientation	Bias introduced by use of incorrect flow model
Meter Geometrical Alteration	Erosion/Corrosion	Negative bias in calculated flow rate
	Buildup of Deposits (Wax, Scale, Asphaltenes, etc.)	Positive bias in calculated flow rate
	Pressure Effects	Depends on instrument
Other Meter Effects	Meter Finish Change (e.g. scale deposits)	Alter discharge coefficient C_d
Fluid Property Changes	Density	Inject flow rate bias
	HC Composition	Affect phase fraction calculation
	Salinity	Affect phase fraction calculation
	Viscosity	Affect phase fraction calculation
	Other additives (H_2O, H_2S…..)	Affect flow and PVT Models

Chapter 4

DETERMINATION OF FLUID FLOW PROFILE

4.1 Introduction

There are several methods available for determining the fluid flow regime for horizontal flow such as Weisman Model, Taitel-Dukler Model, Beggs and Brill Model. This study followed Taitel-Dukler Model for horizontal flow as the assumptions of this model completely matched with existing problem.

4.2 Calculation Approach

In this project, four steps were followed to complete the study on multiphase fluid flow profile and multiphase meter:

- Flow Regime Determination by using Taitel-Dukler Model
- Calculation of Pressure Gradient for Horizontal Pipe
- Investigation for Phase Changes by HYSYS Simulator
- Investigation for Gas Flow Data Accuracy

4.2.1 Flow Regime Determination by using Taitel-Dukler Logical Flow Diagram

This study has been conducted based on the following assumptions [6]:

- Constant gas density
- Isothermal Flow (no thermal effect on density and viscosity)
- Steady state flow

The following parameters are important to determine flow regime:

- Superficial Velocities for Liquid and Gas (U_l and U_g)
- Liquid and Gas Density (ρ_l and ρ_g)
- Liquid and Gas Viscosity (μ_l and μ_g)
- Pipe Diameter (D)
- Pipe Inclination (β)

Table 4.1 Necessary Equations for Taitel-Dukler Model [6]

$\tilde{A}_G = \frac{A_G}{D^2} = \frac{1}{4}\left[arccos(2\tilde{h}_L - 1) - (2\tilde{h}_L - 1)\sqrt{1-(2\tilde{h}_L - 1)^2}\right]$		
$\tilde{A}_L = \frac{A_G}{D^2} = \frac{\pi}{4} - \tilde{A}_G$		
$\tilde{S}_G = \frac{S_G}{D} = arccos(2\tilde{h}_L - 1)$	$\tilde{S}_L = \frac{S_L}{D} = \pi - \tilde{S}_G$	$\tilde{S}_i = \frac{S_i}{D} = \sqrt{1-(2\tilde{h}_L - 1)^2}$
$\tilde{U}_L = \frac{U_L}{U_{LS}} = \frac{\tilde{A}}{\tilde{A}_L}$	$\tilde{U}_G = \frac{U_G}{U_{GS}} = \frac{\tilde{A}}{\tilde{A}_G}$	$\tilde{A} = \frac{\pi}{4}$
$\left(\frac{dP}{dx}\right) gs = \frac{4}{D} C_g \left(\frac{DU_g}{\nu}\right)^{-m} \cdot \frac{1}{2} \rho\, U_g^2$	$\left(\frac{dP}{dx}\right) ls = \frac{4}{D} C_g \left(\frac{DU_l}{\nu}\right)^{-m} \cdot \frac{1}{2} \rho\, U_l^2$	
$X^2 = \frac{(\frac{dP}{dx})ls}{(\frac{dP}{dx})gs}$	$Y = \frac{(\rho_l - \rho_g)\, g \sin\beta}{\left(\frac{dp}{dx}\right)gs}$	

Table 4.2 Factors for Taitel-Dukler Model [6]

Constant for Turbulent Flow C= 0.046,	Exponent for Turbulent Flow, m = 0.2
Constant for Laminar Flow C= 16,	Exponent for Laminar Flow, m = 1
Screening Coefficient, S = 0.01	
Coupling Constant, C_2 = 0.38	

- Now check the following conditions for identifying Flow Regime:

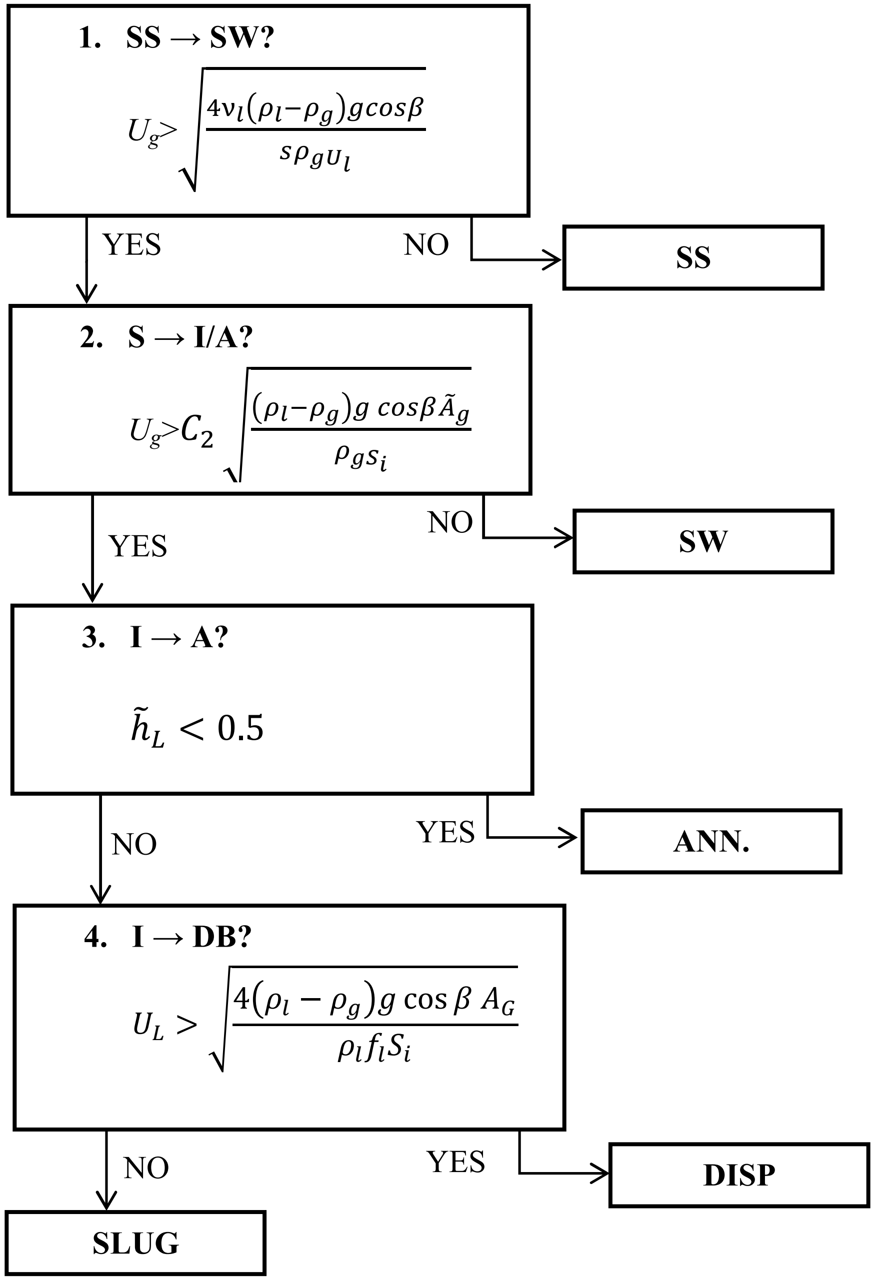

Calculation for BY-1 Well:

Condition:

- Gas Flow Rate: 97.8 MMSCFD
- Condensate Production Rate: 512.3 bbl/d
- Water Production Rate: 191.3 bbl/d
- Pipe ID: 7.625 inch
- Pipe Inclination: 1º
- Gas Density: 0.724 kg/m^3 = 0.04519 lb/ft^3
- Gas Viscosity: 0.0158 cP = 1.06176x10^{-5}lbm/ft-sec (Kinematic Viscosity = 2.34914x10^{-4} ft^2/s)
- Liquid Hydrocarbon Density: 48.71 lb/ft3 (Relative Density = 0.7810)
- Viscosity of Liquid Hydrocarbon: 1.0893 cP = 7.3201x10^{-4}lbm/ft-sec (Kinematic Viscosity = 1.50279x10^{-5} ft^2/s)

Step-1: Calculation of Superficial Reynolds Number for Gas and Liquid Phase

Superficial Gas Velocity, $U_g = \frac{Q_g}{A_g}$

Where,

U_g = Superficial Gas Velocity

Q_g= Gas Flow Rate

A_g = Flowing Cross Section of Gas

$U_g = \frac{97.8\ MMSCF}{D} x \frac{D}{86400\ S} x1000x1000x\ \frac{1}{0.316947\ ft^2}$ = **3571.40 ft/s**

Superficial Liquid Velocity, $U_l = \frac{Q_l}{A_l}$

Total Liquid Rate, Q_l = 512.3 + 191.3 = 703.6 bbl/d = **0.04572 ft^3/s**

So, Superficial Liquid Velocity, $U_l = \frac{0.04572\ ft^3}{S} x \frac{1}{0.316947\ ft^2}$ = **0.14425 ft/s**

Superficial Reynolds Number for Gas Phase = $\frac{D\rho U_g}{\mu}$

= $0.635417\ ft\ x\ \frac{3571.40\ ft}{s}\ x\ \frac{0.04519\ lb}{ft^3}\ x\ \frac{ft-s}{1.06176x10^{-5}lb}$

i.e. **Re = 9659126.37 Turbulent Flow**

Superficial Reynolds Number for Liquid Phase = $\frac{D\rho U_l}{\mu}$

=$0.635417\ ft\ x\ \frac{0.14425\ ft}{s}\ x\ \frac{48.71\ lb}{ft^3}\ x\ \frac{ft-s}{7.3201x10^{-4}\ lb}$

i.e. **Re = 6099.24 Turbulent Flow**

Step-2: Calculation of Superficial Pressure Drop for Gas and Liquid Phase

Superficial Pressure Drop for Gas Phase, $\left(\frac{dP}{dx}\right) gs = \frac{4}{D} C_g \left(\frac{DU_g}{\nu}\right)^{-m} . \frac{1}{2} \rho\ U_g^2$

Where,

$\left(\frac{dP}{dx}\right) gs$ = Superficial Pressure Drop

C_g = Constant for Turbulent Flow = 0.046

ν = Kinematic Viscosity = 0.000234914 ft^2/s

m = Exponent for Turbulent Flow = 0.2

$\left(\frac{dP}{dx}\right) gs =$

$\frac{4}{0.635417\ ft}\ x\ 0.046\ x\ (0.635417\ ft\ x\ 3571.4 \frac{ft}{s} x\ \frac{s}{0.000234914\ ft^2})^{-0.2}\ x\ \frac{1}{2} x \frac{0.04519\ lb}{ft^3}\ x\ 3571.40^2\ \frac{ft^2}{s^2}$

= **3346.01 lb/ft^2-s^2**

Superficial Pressure Drop for Liquid Phase, $\left(\frac{dP}{dx}\right) ls = \frac{4}{D} C_l \left(\frac{DU_l}{\nu}\right)^{-m} . \frac{1}{2} \rho\ U_l^2$

Where,

$\left(\frac{dP}{dx}\right) ls$ = Superficial Pressure Drop

C_l = Constant for Turbulent Flow = 0.046

ν = Kinematic Viscosity = 1.50279x10^{-5} ft2/s

m = Exponent for Turbulent Flow = 0.2

$\left(\frac{dP}{dx}\right) ls$ =

$$\frac{4}{0.635417\ ft}\ x\ 0.046\ x\ (0.635417\ ft\ x\ 0.14425\frac{ft}{s} x\ \frac{s}{1.50279\text{x}10{-}5\ ft^2})^{-0.2}\ x\ \frac{1}{2} x \frac{48.71\ lb}{ft^3}\ x\ 0.14425^2\ \frac{ft^2}{s^2}$$

= **0.025679 lb/ft^2-s^2**

Step-3: Determinationof Liquid Holdup by Using Lockhart-Martinelli Parameter

$$X^2 = \left| \frac{(\frac{dP}{dx})ls}{(\frac{dP}{dx})gs} \right| \qquad Y = \frac{(\rho_l - \rho_g)\ \text{g}\sin\beta}{\left(\frac{dp}{dx}\right)gs}$$

So, $X^2 = \frac{0.025679}{3346.01} = 7.6745x10^{-6}$

X = 0.0028

And $Y = \frac{(48.71 - 0.045198)\ lb}{ft^3}\ x\ \frac{32.714\ ft}{s^2}\ x\ sin1°x\ \frac{ft^2 - s^2}{3346.01\ lb}$

= 0.008

From Figure 3.11, Dimensionless Liquid Fraction, $\widetilde{h_L} = \frac{h_L}{D}$ = 0.02

Step-4: Calculation of Gas and Liquid Fraction

$\tilde{A} = \frac{\pi}{4} = \frac{3.14}{4} = 0.785$

$$\widetilde{A_g} = \frac{1}{4}\left[arccos\left(2\widetilde{h_L} - 1\right) - \left(2\widetilde{h_L} - 1\right)\sqrt{1 - \left(2\widetilde{h_L} - 1\right)^2}\right]$$

$= \frac{1}{4}\left[\arccos(2x0.02-1)-(2x0.02-1)\sqrt{1-(2x0.02-1)^2}\right]$

$= \frac{1}{4}[2.858+0.269]$

= 0.782

$\widetilde{A_l} = \frac{\pi}{4} - \widetilde{A_g}$

$= \frac{\pi}{4} - 0.782$

= 0.003

Step-5: Determination of Flow Regime

- Flow Transition: Stratified Smooth to Stratified Wavy

$$U_g > \sqrt{\frac{4\nu_l(\rho_l-\rho_g)g\cos\beta}{s\rho_g u_l}}$$

$$U_g > \sqrt{\frac{4x1.50279x10-5x(48.71-0.045198)x32.174x\cos 1°}{0.01x0.045198x0.14425}}$$

$$U_g > \sqrt{\frac{0.0941}{6.5198x10^{-5}}}$$

$U_g >$ 37.99 [where, U_g = 3571.40 ft/s]

So the flow may be Intermittent or Annular

- **Flow Transition:** Stratified to Intermittent or Annular

$$\tilde{S}_i = \sqrt{1-(2\tilde{h}_L-1)^2}$$

$$= \sqrt{1-(2x0.02-1)^2} = 0.28$$

$$U_g > C_2\sqrt{\frac{(\rho_l-\rho_g)g\cos\beta\tilde{A}_g}{\rho_g s_i}}$$

$$U_g > 0.38x\sqrt{\frac{(48.71-0.045198)x32.174x\cos 1°x0.782}{0.045198x0.28}}$$

$U_g > 310.48$ [where, U_g = 3571.40 ft/s]

This result confirms that flow is not stratified wavy; it may be intermittent or annular.

- **Flow Transition: Intermittent to Annular Flow**
  If $\widetilde{h_L} < 0.5$ then flow will be annular, otherwise it may be Dispersed Bubble Flow or Slug Flow. But in this case it is found $\widetilde{h_L}$ = 0.02 which is less than 0.5

So Flow Regime is found to be Annular. Using the corresponding data set and similar calculation steps, results for all seven wells were determined that is presented in the next section.

Results Summary

Table 4.3 and Table 4.4 summarize the results of all calculated parameters for determining the fluid flow profile at actual flow rate condition.

Table 4.3 Calculated results for determining fluid flow profile

Well No	Gas Rate (MMSCFD)	Condensate Rate (bbl/d)	Water Rate (bbl/d)	Superficial Gas Velocity (ft/s)	Superficial Liquid Velocity (ft/s)	Gas Density (lb/ft^3)	Gas Viscosity (cP)	Liquid Density (lb/ft^3)	Liquid Viscosity (cP)
BY-1	97.8	512.3	191.3	3571.40	0.14425	0.045198	0.0158	48.71	1.0893
BY-2	65.1	669.2	6.8	2377.28	0.13860	0.045385	0.0129	48.71	1.0893
BY-3	69.1	855.7	9.1	2523.35	0.17730	0.046385	0.0129	47.20	1.0788
BY-4	47	419	7.5	1716.32	0.08745	0.046484	0.0130	47.27	1.0865
BY-5	62.1	718.6	10.9	2267.73	0.14957	0.046883	0.0130	47.27	1.0865
BY-6	57.9	332	7.4	2114.36	0.06959	0.046696	0.0125	47.20	1.0788
BY-7	63.8	469.9	9.9	2329.81	0.09837	0.045198	0.0124	47.20	1.0788

Table 4.4 Calculated results for determining fluid flow profile

Well No	Re for Gas	$\left(\frac{dP}{dx}\right)gs$	Re for Liquid	$\left(\frac{dP}{dx}\right)ls$	X	Y	$\widetilde{h_L}$	$\widetilde{A_g}$	$\widetilde{A_l}$	SS to SW Transition	S to I/A Transition	Flow Regime
BY-1	9659126.37	3346.01	6099.24	0.025679	0.0028	0.008	0.02	0.782	0.003	$37.99<U_g<\tilde{h}_L$	$310.48<U_g<\tilde{h}_L$	**Annular**
BY-2	7908471.82	1549.47	5860.35	0.023894	0.0039	0.018	0.02	0.782	0.0037	$38.68<U_g<\tilde{h}_L$	$304.10<U_g<\tilde{h}_L$	**Annular**
BY-3	8579359.21	1755.38	7335.39	0.036229	0.0045	0.015	0.02	0.782	0.0037	$33.66<U_g<\tilde{h}_L$	$296.09<U_g<\tilde{h}_L$	**Annular**
BY-4	5802924.92	880.03	3597.34	0.010176	0.0034	0.030	0.021	0.781	0.0040	$48.05<U_g<\tilde{h}_L$	$292.13<U_g<\tilde{h}_L$	**Annular**
BY-5	7733081.65	1463.04	6153.01	0.026741	0.0043	0.018	0.02	0.782	0.0037	$36.58<U_g<\tilde{h}_L$	$294.74<U_g<\tilde{h}_L$	**Annular**
BY-6	7468565.34	1275.61	2878.85	0.006728	0.0023	0.021	0.02	0.782	0.0037	$53.55<U_g<\tilde{h}_L$	$295.11<U_g<\tilde{h}_L$	**Annular**
BY-7	8029845.05	1477.57	4069.75	0.012546	0.0029	0.018	0.02	0.782	0.0037	$45.78<U_g<\tilde{h}_L$	$299.96<U_g<\tilde{h}_L$	**Annular**

Table 4.5 and Table 4.6 summarize the results of all calculated parameters for determining the fluid flow profile at reduced flow condition where flow was reduced from 30 MMSCFD to 45 MMSCFD.

Table 4.5 Calculated results for determining fluid flow profile

Well No	Gas Rate (MMSCFD)	Condensate Rate (bbl/d)	Water Rate (bbl/d)	Superficial Gas Velocity (ft/s)	Superficial Liquid Velocity (ft/s)	Gas Density (lb/ft^3)	Gas Viscosity (cP)	Liquid Density (lb/ft^3)	Liquid Viscosity (cP)
BY-1	60	176.8	5.76	2191.04	0.037430	0.045198	0.0158	48.71	1.0893
BY-2	30	308.6	2	1095.52	0.063682	0.045385	0.0129	48.71	1.0893
BY-3	20	269.3	2.1	730.35	0.055645	0.046385	0.0129	47.20	1.0788
BY-4	26	231.4	3.4	949.45	0.048141	0.046484	0.0130	47.27	1.0865
BY-5	20	223.4	2.1	730.35	0.046234	0.046883	0.0130	47.27	1.0865
BY-6	25	160.8	2.1	912.93	0.033399	0.046696	0.0125	47.20	1.0788
BY-7	30	219.5	3.9	1095.52	0.045804	0.045198	0.0124	47.20	1.0788

Table 4.6 Calculated results for determining fluid flow profile

Well No	Re for Gas	$\left(\frac{dP}{dx}\right)gs$	Re for Liquid	$\left(\frac{dP}{dx}\right)ls$	X	Y	$\widetilde{h_L}$	$\widetilde{A_g}$	$\widetilde{A_l}$	SS to SW Transition	S to I/A Transition	Flow Regime
BY-1	7288917.74	1337.86	1582.64	0.002171	0.0013	0.020	0.018	0.7822	0.0032	$74.43<U_g<\tilde{h}_L$	$312.80<U_g<\tilde{h}_L$	Annular
BY-2	3644458.87	384.20	2692.64	0.005893	0.0039	0.071	0.022	0.7811	0.0043	57.06	$296.37<U_g<\tilde{h}_L$	Annular
BY-3	2483173.22	188.44	2302.06	0.004499	0.0049	0.141	0.023	0.7808	0.0046	60.09	$285.11<U_g<\tilde{h}_L$	Annular
BY-4	3210130.27	303.16	1980.43	0.002786	0.0030	0.088	0.0235	0.7806	0.0048	64.76	$283.36<U_g<\tilde{h}_L$	Annular
BY-5	2490526.72	190.35	1901.99	0.002675	0.0037	0.139	0.0235	0.7806	0.0048	65.80	$282.50<U_g<\tilde{h}_L$	Annular
BY-6	3224770.74	281.31	1381.75	0.001919	0.0026	0.094	0.022	0.7811	0.0043	77.30	$287.61<U_g<\tilde{h}_L$	Annular
BY-7	3775791.08	379.92	1894.92	0.002632	0.0026	0.070	0.0218	0.7811	0.0043	67.09	$293.07<U_g<\tilde{h}_L$	Annular

From Table 4.3 and Table 4.4, all wells were flowing at actual flow condition. It is found by Superficial Reynolds number that Gas Flow and Liquid Flow both were turbulent. Flow transition check calculation shows that all values are less than Superficial Gas Velocity and dimensionless liquid fractions are also less than 0.5. So from Taitel and Dukler Model it can be concluded that flow is annular.

Table 4.5 and Table 4.6 summarizes the calculated results at reduced flow condition, the reason behind this calculation is as time goes the reservoir will deplete and gas composition will change, so flow regime may change due to changing condition and if flow regime is changed that may lead to increase uncertainty level of multiphase flow meter. At that condition again flow regime calculation has been done and found transition flow values are more or less similar which is 57 to 74 for stratified smooth to stratified wavy and 282 to 313 for intermittent/annular flow transition, while actual flow condition these were 33 to 53 and 292 to 310 respectively, which are less than Superficial Gas Velocity and also dimensionless liquid fraction is less than 0.5 and as per Taitel and Dukler Model, flow is annular

4.2.2 Calculation for Pressure Gradient in Horizontal Pipe

This calculation was performed for horizontal pipeline from downstream of choke valve to production header. This pipeline is about 200 ft where pressure drop is minimum (approximately 5 psi), study carried out to understand the pressure gradient profile for all 7 wells of North Pad. To design a two-phase pipeline, an accurate assessment of pressure drop and liquid holdup is necessary, and the results of this study can be used for future reference.

Necessary Equations:

- Average dimensionless Pressure Gradient, $\Delta P^* = \frac{\Delta P}{\rho_m g L}$
- Mixture Reynolds number, $Re_m = \frac{D U_m \rho_m}{\mu_m}$
- Mixture Froude number, $Fr_m = \frac{U_m^2}{gL}$
- Mixture Density, $\rho_m = \lambda_L \rho_L + (1 - \lambda_L)\rho_g$
- Mixture Viscosity, $\mu_m = \lambda_L \mu_L + (1 - \lambda_L)\mu_g$
- Mixture Velocity, $U_m = U_l + U_g$
- Where, $\lambda_L = \frac{U_l}{U_m}$

$$\lambda_L = \frac{0.14425}{3571.40 + 0.14425} = 4.03887x10^{-5}$$

Mixture Density, $\rho_m = (4.03887x10^{-5}x48.71) + \left((1 - 4.03887x10^{-5})x0.04519\right)$

$= 0.0473505 lb/ft^3$

Mixture Viscosity, $\mu_m = (4.03887x10^{-5}x7.3201x10^{-4}) + ((1 - 4.03887x10^{-5})x1.06176x10^{-5})$

$= 8.69801x10^{-6} lbm/ft\text{-}sec$

Pipe Length from Choke Valve to Production Manifold = 200 ft

Average Pressure Drop = 5 psi [From Field Data]

So, Dimensionless Average Pressure Gradient, $\Delta P^* = \frac{5}{0.0473505x32.174x200}$

$= \underline{0.0164}$

Results Summary

Table 4.7 Pressure Gradient Result of Wellhead Flow Line

Well no	Mixture Velocity, ft/s	Holdup	Mixture Density, lb/ft^3	Mixture Viscosity,lbm/ ft-sec	Reynolds Number	Pressure Gradient
BY-1	3571.54	$4.039x10^{-5}$	0.0473505	$8.69801x10^{-6}$	148251915.10	0.01640
BY-2	2377.42	$5.830x10^{-5}$	0.0482221	$8.71097x10^{-6}$	100351737.90	0.01611
BY-3	2523.53	$7.026x10^{-5}$	0.0496980	$8.71913x10^{-6}$	109676470.70	0.01563
BY-4	1716.41	$5.095x10^{-5}$	0.0488900	$8.77275x10^{-6}$	72936413.42	0.01589
BY-5	2267.88	$6.595x10^{-5}$	0.0499974	$8.78358x10^{-6}$	98431963.35	0.01554
BY-6	2114.43	$3.291x10^{-5}$	0.0482479	$8.42358x10^{-6}$	92345276.74	0.01610
BY-7	2329.91	$4.222x10^{-5}$	0.0471889	$8.36306x10^{-6}$	100242882.20	0.01647

For pressure gradient calculation, individual flow line is considered only because all individual flow lines are 8 inches diameter, connected to 20 inches production header and then goes to South Pad separator. At production header, all fluid streams of 7 wells are combined where fluid composition and flow pattern will be different from individual well flow. This production header is about 4.5 km long and pressure drop is higher than shorter flow line, so pressure gradient must be higher than these shorter flow lines. Table 4.7 summarizes the calculated results of all 7 flow lines.

Dimensionless Average Pressure Gradient values are from 0.01554 to 0.01647 which are very close to each other.

4.2.3 Investigation for Phase Changes by HYSYS Simulator

HYSYS, a Process Engineering simulation tool, is widely used in universities and industries for research, development, modeling and design. HYSYS serves as the engineering platform for modeling processes in Gas processing, Refining and Chemical processes. Here HYSYS was used to find the phase envelope at three points such as before choke valve, after choke valve and separator outlet. In steady state mode, well head stream after choking by valve it goes to the separator and divides into its constituent vapor and liquid phases. The vapor and liquid in the vessel are allowed to reach equilibrium, before they are separated.

The entire simulation study and analysis was done on ASPEN^{TM} HYSYS 3.2. For simulation, fluid package was selected as Peng-Robinson model. The main reason behind this, for oil, gas and petrochemical applications, the Peng-Robinson is generally the recommended and widely accepted property package. ASPEN HYSYS contains an oil manager which organizes the data and HYSYS properties were used for property generation of the streams. [15].

Figure 4.1 in the next page shows the Flow Model and the main purpose is to find out phase envelope at every pressure drop down point through HYSYS simulation.

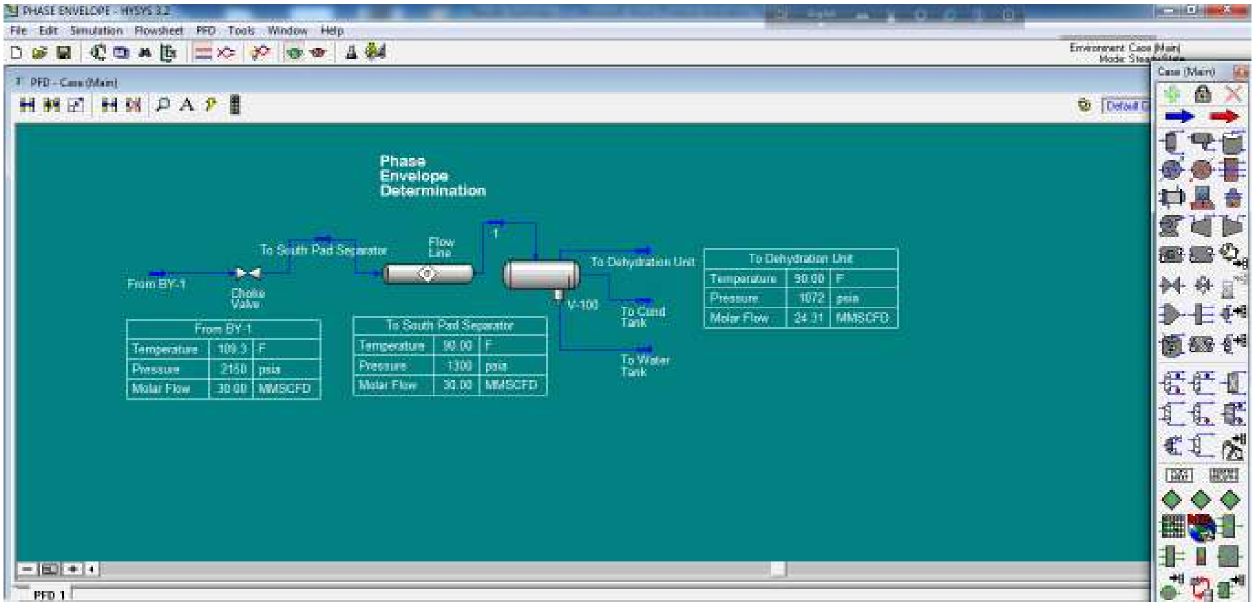

Figure 4.1 Flow Model for Phase Envelope Determination by HYSYS

In this HYSYS Model (Figure 4.1), fluid stream is flown through choke valve at 97.8 MMSCFD rate and pressure dropped down from 2150 psi to 1300 psi, temperature changes from 109.3º F to 90º F. This choked flow further goes to separator for primary separation through flow line. This flow rate is then reduced to 30 MMSCFD to investigate that fluid composition and phase envelope is changing or not and phase envelope is determined for three points such as before choke valve, after choke valve and after separator.

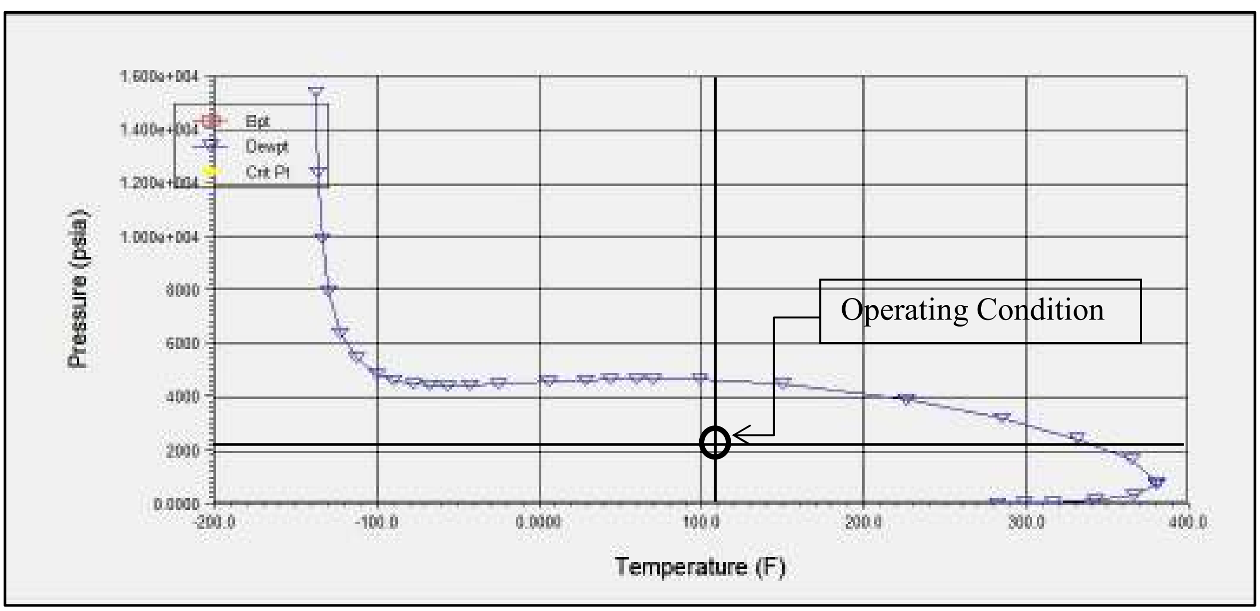

Figure 4.2: Phase Envelope before Choke Valve for 30 MMSCFD Flow Rate

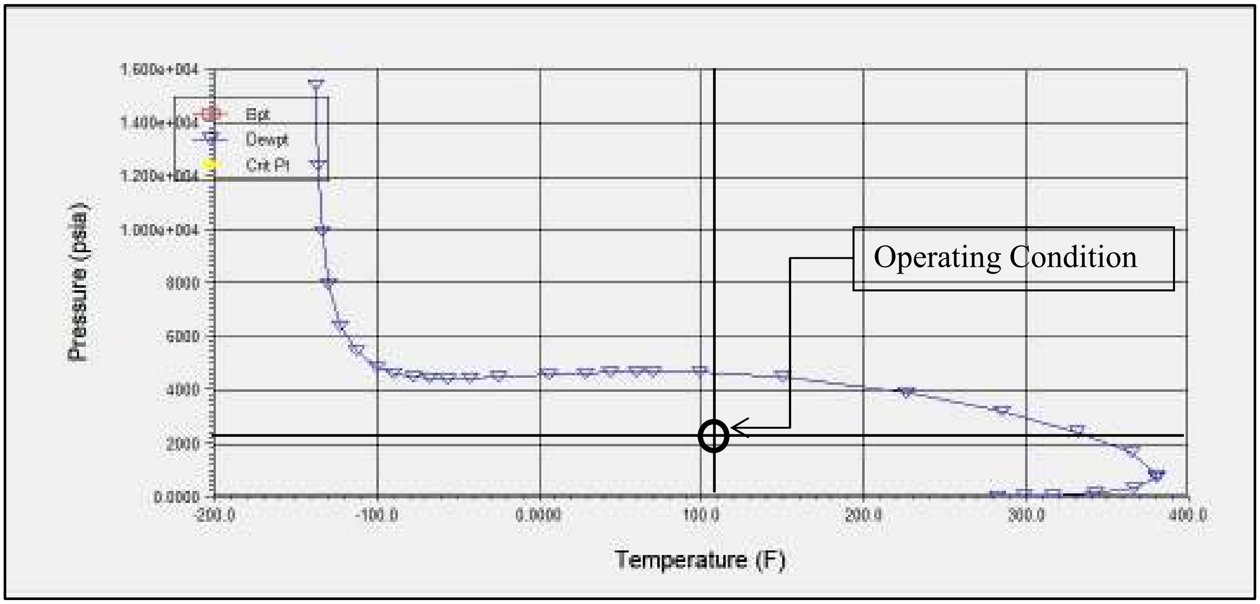

Figure 4.3 Phase Envelope before Choke Valve for 97.8 MMSCFD Flow Rate

Figure 4.2 and Figure 4.3 illustrates the phase envelope for 30 MMSCFD and 97.8 MMSCFD flow rate respectively, their operating pressure and temperature are 2150 psi and 109.3º F. It is observed that at both flow conditions operating points are within phase envelope and at same position, their operating point indicates that fluid stream contains more liquid to knock out and their position is not changed due to change in flow rate.

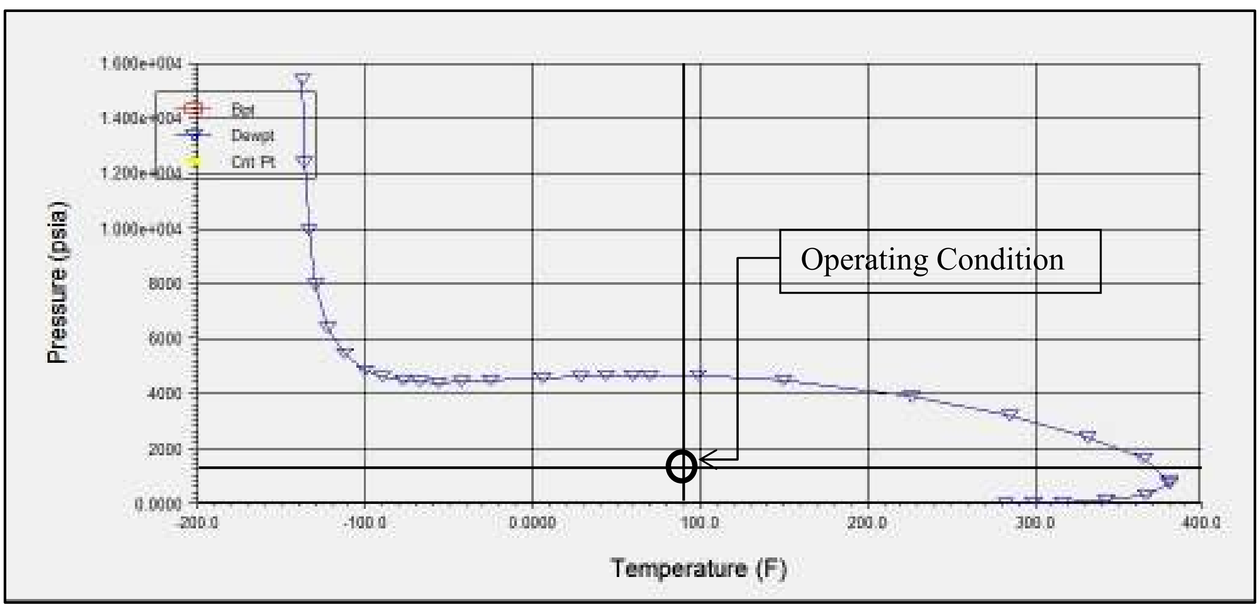

Figure 4.4 Phase Envelope after Choke Valve for 30 MMSCFD Flow Rate

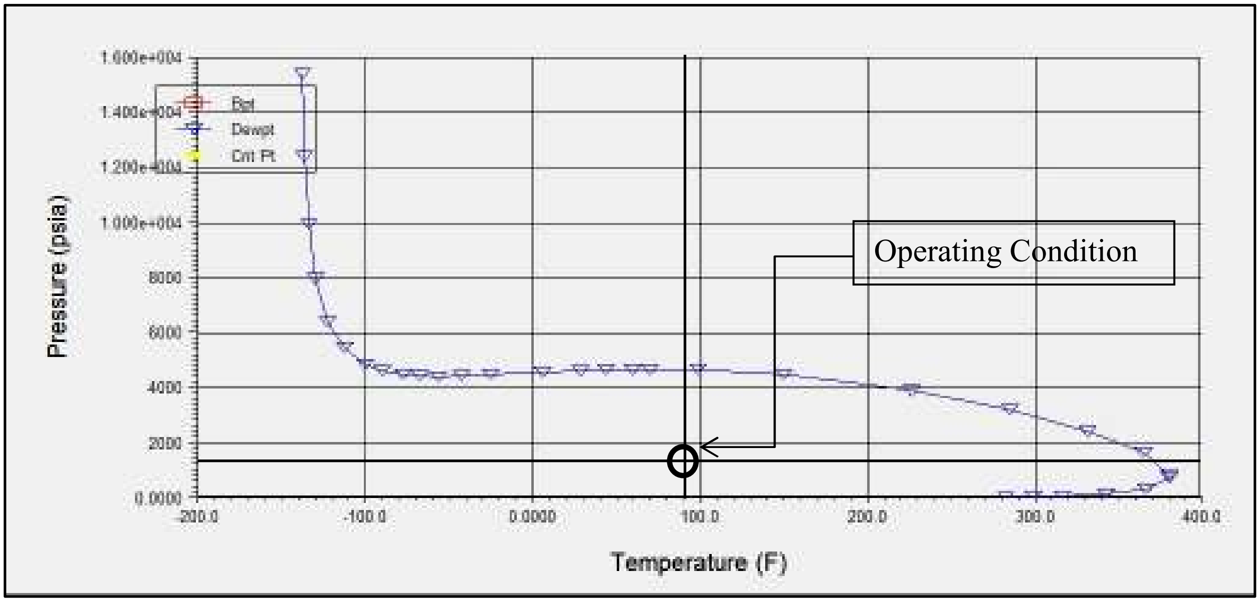

Figure 4.5 Phase Envelope after Choke Valve for 97.8 MMSCFD Flow Rate

Figure 4.4 and Figure 4.5 illustrates the phase envelope for 30 MMSCFD and 97.8 MMSCFD flow rate respectively. Their operating pressure and temperature are 1300 psi and 90º F. It is found from the figure that at both flow conditions, operating points are within phase envelope and at same position; their operating point indicates that fluid stream contains more liquid to knock out and their position is not changed due to flow change. It is also found that phase envelope of before and after the choke valve is not changed due to flow rate and pressure changes.

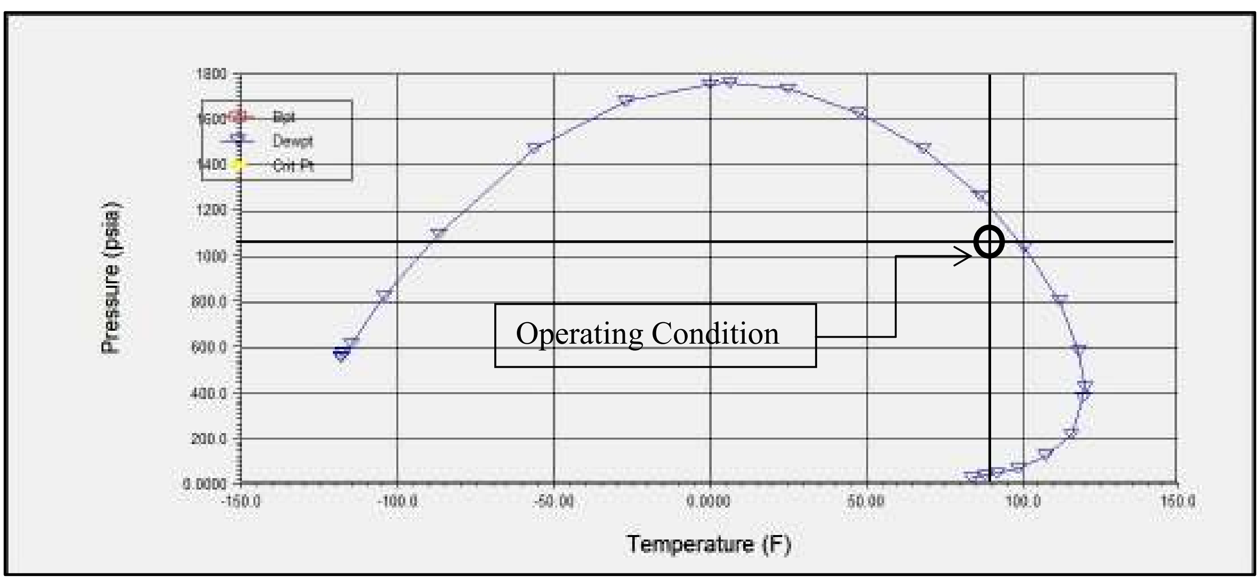

Figure 4.6 Phase Envelope at Separator Outlet for 30 MMSCFD Flow Rate

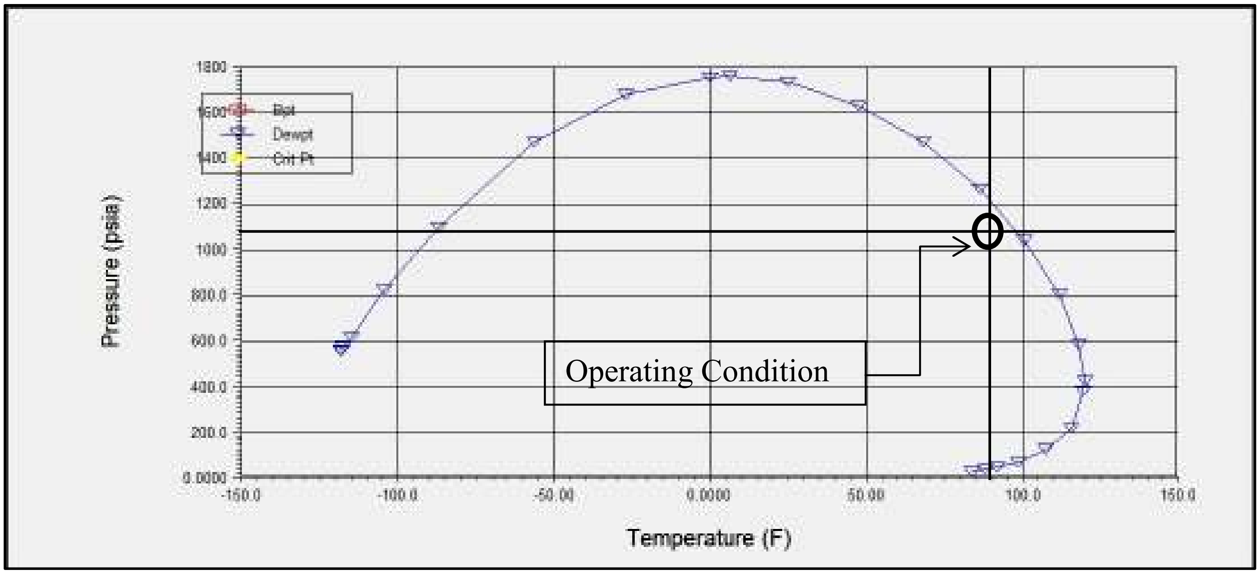

Figure 4.7 Phase Envelope at Separator Outlet for 97.8 MMSCFD Flow Rate

Figure 4.6 and Figure 4.7 illustrates the phase envelope for 30 MMSCFD and 97.8 MMSCFD flow rate respectively, their operating pressure and temperature are 1072 psi and 90º F. Both figure shows that operating points are still within phase envelope and operating point exist near bubble point line but they are different from the phase envelope of before and after choke valve condition because some primary separation occurs at separator. Though the shape of phase envelope is changed from previous condition and operating point also shifted but still this fluid stream has liquids to knock out which will be further separated by dehydration unit.

This project does not find any change in phase envelope for two different flow conditions.

4.2.4 Investigation for Gas Flow Data Accuracy

Gas flow rate accuracy is very important for production allocation, well testing and for reservoir management. As per manufacturer's recommendation meter accuracy will be within ±5% and this project investigated the measurement formula whether it matches the recommended guideline or not. To carry out this investigation V-Cone differential pressure formula was used.

To measure Gas Flow Rate following V-Cone Differential Pressure Formula was used [11]:

$$Q_g = \frac{\pi D^2}{4} \frac{C_D y}{\varphi_g} \sqrt{\frac{2.\Delta P.\rho_g}{\beta^{-4} - 1}}$$

$$\varphi_g^2 = 1 + CX + X^2$$

$$y = 1 - (0.649 + 0.696.\beta^4)\frac{0.0360912.\Delta P}{K.P}$$

Where,
Q_g = Volumetric Flow Rate, MACFD
C_D = Discharge Coefficient = 0.80
y = Fluid Expansibility Factor
φ_g= 2-phase multiplier
X = Lockhart-Martinelli Factor
K = Specific Heat Ratio = $\frac{C_P}{C_V} = 1.29$
P = Operating Pressure
β = Beta ratio = $\sqrt{1 - \frac{d^2}{D^2}}$ = 0.70
ΔP = Differential Pressure, inWC

Sample Calculation for BY-1:

$$y = 1 - (0.649 + 0.696.\,0.70^4)\frac{0.0360912x14}{1.29x1250} = \underline{0.9997}$$

Where, $\Delta P = 14.5"H_2O$, Operating Pressure, $P = 1300\ psi$

$$\varphi_g^2 = 1 + CX + X^2$$

$$\varphi_g = \sqrt{1 + 20x0.0028 + 0.0028^2} = \underline{1.0276}$$

$Where, X = 0.0028\ determined\ earlier\ section\ of\ calculation\ step\ for\ BY - 1$

$$Q_g = \frac{\pi x 5.761^2}{4}\frac{0.8x0.9997}{1.0276}\sqrt{\frac{2x16x0.045198}{0.70^{-4}-1}} = 14.83\ ACFS = 106.40\ MMSCFD$$

While flow meter showing 97.8 MMSCFD at 14.5”H_2O DP

Error = $\frac{106.40-97.8}{97.8}x100\% = \mathbf{8.79}\%$

This calculation was carried out for seven wells determining flow meter reading error percentage in all seven wells. The results are presented next.

Results Summary

Table 4.8 Calculated Results for Meter Data Accuracy

Well No	Actual Flow, MMSCFD	Flowing Pressure, psig	y	φ_g	DP (wc)	Calculated Flow, MMSCFD	Error %
BY-1	97.8	1300	0.9997	1.0276	14.5	106.40	8.79
BY-2	65.1	1270	0.9998	1.0385	11.3	69.61	6.93
BY-3	69.1	1270	0.9998	1.0444	11.7	73.58	6.48
BY-4	47	1250	0.9998	1.0335	10.0	50.86	8.22
BY-5	62.1	1250	0.9998	1.0419	11.0	66.22	6.63
BY-6	57.9	1250	0.9998	1.0227	10.8	62.25	7.51
BY-7	63.8	1260	0.9998	1.0287	11.1	68.27	7.01

Table 4.8 summarizes the calculated results for determining meter accuracy percentage for wells 1-7, where minimum value is 6.48% for BY-3 well and maximum value is 8.79% for BY-1 well, where meter flow and actual flow for BY-3 was 69.1 MMSCFD and 73.58 MMSCFD respectively, similarly for BY-1 it was 97.8 MMSCFD and 106.4 MMSCFD respectively.

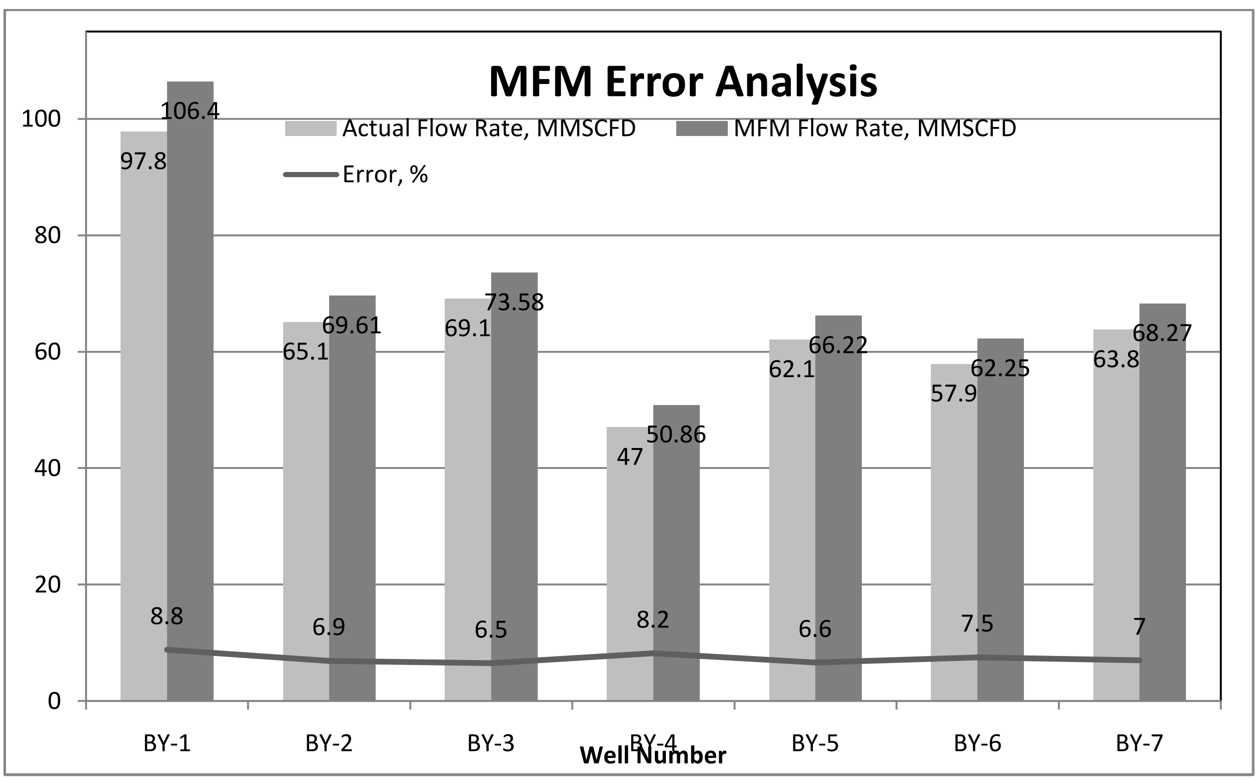

Figure 4.8 MFM Error Trend Analysis

Figure 4.8 illustrates the actual flow, meter flow and error percentage of multiphase meter of BYGP North Pad. Error percentage for BY-1 is 8.79% for 97.8 MMSCFD flow rate and for BY-4 is 8.22% where for 47 MMSCFD flow rate is minimum among 7 wells of North Pad and minimum error percentage is for BY-3 is 6.48% where flow rate where flow rate is 69.1 MMSCFD. From this trend it has been concluded that there is no linear relationship with flow rate of each well.

4.3 Applicability of MFM in Bangladesh

Advantages of Multiphase Flow Meter:

- It can measure the unprocessed well streams very close to the well.
- It can handle complex flows compared to single phase measurement system.
- Initial installation cost is low compare to Test Separator System.
- It can provide continuous monitoring of well performance and thereby better reservoir exploitation/drainage.
- Less space is required and suitable for offshore applications.
- Low maintenance cost.
- Easily replaceable.

Disadvantages of Multiphase Flow Meter:

- High measurement uncertainty compare to single phase metering.
- Complex technology.
- No standard and simple method for multiphase fluid sampling is yet available. Gas composition data need to input its PVT Software on regular basis, if gas sampling cannot be done accurately then there is a chance to input wrong data and finally measurement uncertainty will increase [16].

Bibiyana Gas Field first introduced MFM in Bangladesh. Except this field, all other fields are using single phase measurement system and conventional Test Separator System for Well Testing. This system requires the constituents or “phases” of the well streams to be fully separated upstream of the point of measurement. To accomplish this stabilized flow, more capital investment is required where MFM offers an attractive alternative choice which will not increase installation cost, moreover it will reduce the cost and will provide in line multiphase flow rate continuously. But this MFM has two major limitations, one is measurement uncertainty and other is no established multiphase fluid sampling procedure is in place.

If there is space constraint then MFM can be installed but before making any decision to install a MFM in any Bangladeshi field, it should consider the following things:

- Due to increased uncertainty, Cost-Benefit Analysis should be performed over the life cycle of the project to justify its application.
- First investigate and describe the expected flow regime from the wells to be measured and determine the production envelope before selecting optimum multiphase metering technology.
- Most of the available MFM in the market needs update on some fluid properties such as density, permittivity, conductivity salinity on regular basis, taking care of this in mind is important.
- Careful comparison and selection procedure is required because a number of different MFM's are available in the market, employing a great diversity of measurement principles and solutions. Some MFM's work better in certain applications than others.
- Need to consider of MFM's capability of continuously measuring the representative phases and volumes within the required uncertainties. The well stream flow rates will vary over the life time of the well and it is important to ensure that the MFM will measure with the required uncertainty at all times.
- Type of MFM is another important factor. In addition the installation must include adequate auxiliary test facilities to allow calibration and verification during operation to ensure confidence in the measurements over the well life time.
- Due to the higher measurement uncertainties, it is generally not recommended to use a multiphase flow meter to replace a high accuracy fiscal measurement.

Chapter 5

CONCLUSIONS AND RECOMMENDATIONS

5.1 Conclusions

Based on the objectives of this project to investigate Multiphase Metering Systems and Measuring Accuracy, the following conclusions are made from this study:

- Calculation has been done based on PVT properties to identify fluid flow regime and it is found that the flow is annular.
- This project has investigated for phase changes in individual flow lines for actual and reduced flow rate condition and simulation study suggests no phase changes will occur while flow rate will be declined.
- Working principle of multiphase flow meter has been studied and found it is completely matched with calculated results and fluid flow regimes though it has some inaccuracy. At constant error this meter can be used for online monitoring.
- Manufacturer's data sheet shows that this flow meter works well for 43.5 to 45.1 lb/ft^3 Oil density and 1.15 to 4.46 lb/ft^3 Gas density, where calculated gas and oil density of North Pad Well is 0.05 lb/ft^3 and 48.71 lb/ft^3 respectively. This improper density range is a possible cause of meter error.
- This study found gas flow rate reading by the meters is higher than actual value by 6.6% to 8.8% and there is no linear relation with flow rate and it is unpredictable to forecast about future uncertainty level. Due to uncertainty it is not recommended for fiscal metering but compare to lower installation and maintenance cost with test separator system and for space limitations it can be used for well surveillance.
- There is inline calibration option for this multiphase flow meter; PVT data, water fraction, water conductivity and fluid composition data need to be updated regularly for getting accurate meter data. This project does not find any standard sampling procedure to collect fluid stream sample. There is sample point before and after the meter and currently sample is collected through this point and study found that this sampling and lab analysis is a challenging task because there is no phase equilibrium of fluid stream at sampling zone and each phase collected contains some fraction of the other. This mixed phase leads to improper lab analysis and wrong input to meter.
- To verify the correctness of water flow rate measurement from the meter or if the microwave measurement fails, there is an option to use gamma densitometer but it was not consider during design phase.

- Compared to capital investment and maintenance cost this meter is an excellent choice for well surveillance only but before doing this it should ensure that uncertainty limit are fixed; that means uncertainty level must not be changed with the entire life of the well.

5.3 Recommendations

From the study, this project recommends the following things:

- Need to develop a standard and simple multiphase fluid sampling procedure.
- Need to check measurement uncertainty within limit regularly.
- Calibrate the Flow Meter on regular basis.
- For new installation, greater care should be taken, especially on meter type, cost-benefit analysis, flow regime, calibration facility and cost of the unit.
- This meter can be used for measuring the process parameters but should not be wise to use custody transfer metering.

REFERENCES

1. *Process Description and Control Narrative,*Bibiyana Gas Field, Chevron Bangladesh Ltd., 2007.
2. Theuveny, B.C., Segral, G., and Pinguet, B., "*Multiphase Flowmeters in Well Testing Applications",* SPE Annual Technical Conference and Exhibition, New Orleans, Lousiana, 30th September-3rd October 2001.
3. Installation and Operation Manual of RFM Wet Gas Meter, Chevron Bangladesh Ltd., Revision B, 2007.
4. *Handbook of Multiphase Flow Metering*, Norwegian Society for Oil and Gas Measurement (NFOGM) and The Norwegian Society of Chartered Technical and Scientific Professionals (Tekna), Revision 2, March 2005.
5. API Recommended Practice for Measurement of Multiphase Flow (API RP86), First Edition, September 2005.
6. Time, Rune W., "*Two Phase Flow in Pipelines*", Course Compendium, Department of Petroleum Engineering, University of Stavanger, January 1, 2009.
7. Newton, C.H., Bhardwaz, M. and Behnia, M., "*Effects of Pipe Diameter on Pressure Drop Calculationsin Horizontal Two Phase Flow",* 11th Australasian Fluid Mechanics Conference , University of Tasmania, Hobart, Australia, 14-18 December 1992.
8. Falcone, G. and Teodoriu, C., Reinicke, K.M., Bello, O.O., and Clausthal, TU., *Multiphase-Flow Modeling Based on Experimental Testing: An Overview of Research Facilities Worldwide and the Need for Future Developments,* SPE Projects, Facilities and Construction Journal, Volume 3, Number 3, pp. 1-10., 2008
9. Omebere-Iyari, N. K., Azzopardi, B. J. and Ladam, Y.(2007) "*Two-phase flow patterns in large diameter vertical pipes at high pressures*", The AIChE Journal, Volume 53(10), pp. 2493-2504.
10. Cheng, H., Hills, J. H. and Azzopardi, B. J. (1998) "*A study to bubble-to-slug transitions in the vertical gas-liquid flow in columns of different diameter*", International Journal of Multiphase flow, Volume 24(3), pp. 431-452.
11. Nyfros, E., Loland, T., Coupot, J. and Lund Bo, O.,*New Compact Wet Gas Meter Based on a Microwave Water Detection Technique and Differential Pressure Flow Measurement,* North Sea Flow Measurement Workshop, 22-25th October 2002.
12. Tosic, S.and Medhizadeh, P., *Multiphase Well Rate Measurements Applied to Reservoir Analysis,* Abu Dhabi International Petroleum Exhibition and Conference, 3-6 November 2008.
13. Cellos, H., and Wee, A. ,"*Multiphase Flow Measurement System of High-GOR Applications",* SPE Western Regional Meeting, Anchorage, Alaska, 26-28 May 1999.
14. C. Correa Feria, R., "*An In-House Experiment about PVT Impact on Multiphase Metering Accuracy",* SPE Latin American and Caribbean Petroleum Engineering Conference, Lima, Peru, 1-3 December 2010.

15. Aspen HYSYS, version 3.2 (build 5029); Hyprotech Ltd.
16. Hollaender, F., Zhang, J. J., Pinguet, B., Bastos, V. and Delvaux, E., *An Innovative Multiphase Sampling Solution at the Well Site to Improve Multiphase Flow Measurements and Phase Behavior Characterization,* International Petroleum Technology Conference, Dubai, 4-6 December, 2007.

APPENDIX - A

Gas Analysis Report

Sampling Date: 20/11/2012 Time: 14:00 hr Analysis Date: 22/11/2012
Sample Location: At BY#1 Wellhead
Temp: N/A
Pressure: N/A Sampled by: Chevron

Table A-1: Wellhead Gas Analysis Report of November 2012

Component	% Mole	% Vol
Nitrogen	0.20117	0.201
CO_2	0.14019	0.140
Methane	95.82575	95.825
Ethane	2.32951	2.330
Propane	0.71803	0.718
i-Butane	0.21230	0.212
n-Butane	0.17959	0.180
i-Pentane	0.10066	0.101
n-Pentane	0.05341	0.053
Hexane	0.06763	0.068
Heptane	0.10107	0.101
Octane	0.06484	0.065
Nonane+	0.00584	0.006
Total	**100**	**100**

Physical Properties: (Method: ASTM D 3588-98, GPA Standard 2172-96)
SG: 0.591130
Gross Heating Value: 1059.30 BTU/SCF
Viscosity: 0.023 cP

GOR Oil Analysis Report

Sampling Date: 29/10/2007 Time: 14:00 hr Analysis Date: 11/11/2007
Sample Location: At BY#1 Wellhead
Temp: N/A
Pressure: N/A Sampled by: Chevron and BUET

Table A-2: Wellhead Oil Analysis Report of November 2007

Component	% Mole	% Wt
Ethane	0.0	0.0
Propane	0.0	0.0
i-Butane	0.0	0.0
n-Butane	0.0	0.0
i-Pentane	0.0	0.0
n-Pentane	0.64	0.32
Hexane	7.64	4.51
Heptane	21.91	14.89
Octane	24.56	19.08
Nonane	4.07	3.73
Decane	7.99	8.12
C11	3.96	4.42
C12	3.70	4.50
C13	3.77	4.96
C14	3.47	4.91
C15	6.83	10.38
C16	4.51	7.28
C17	1.81	3.11
C18	2.03	3.68
C19	1.56	3.00
C20	1.54	3.11
Total	100	100

Mole wt. of Oil (gm/mole): 140.0425

Well-Head Gas Stream Analysis Report

Sampling Date: 29/10/2007 Time: 14:00 hr Analysis Date: 11/11/2007
Sample Location: At BY#1 Wellhead
Temp: N/A
Pressure: 3118 psi Sampled by: Chevron and BUET

Produced Gas in Liter (14.696 psiaand 0°C): 15.9465
Produced Oil in gram at 30°C: 0.953
Density of Oil in gm/cc at 30°C: 0.827
Produced Water in gram at 30°C: 0.633

Table A-3: Wellhead Gas Stream Analysis Report of November 2007

Component	% Mole	% Wt
Nitrogen	0.294	0.451
CO_2	0.065	0.156
Methane	90.380	79.366
Ethane	2.237	3.682
Propane	0.686	1.655
i-Butane	0.205	0.653
n-Butane	0.172	0.547
i-Pentane	0.092	0.365
n-Pentane	0.073	0.288
Hexane	0.200	0.944
Heptane	0.295	1.617
Octane	0.231	1.447
Nonane	0.037	0.258
Decane	0.072	0.562
C11	0.036	0.306
C12	0.033	0.312
C13	0.034	0.343
C14	0.031	0.340
C15	0.062	0.716
C16	0.041	0.504
C17	0.016	0.215
C18	0.018	0.254
C19	0.014	0.207
C20+	0.014	0.215
H_2O	4.661	4.596
Total	100	100

C7+ Mol wt. (gm/mole): 142.626
Gas Stream Mol wt. (gm/mole): 18.269

APPENDIX - B

Multiphase Flow Meter Data Sheet

RFM Wet Gas Meter
Topside Version

INSTRUMENT DATA SHEET

Serial No.: WGM-1017-05 to WGM-1023-05

Project no.:	55321003	Customer:	Unocal Bangladesh
Doc No/Rev.:	TCE 005213/B	P.O. No.:	UBBTL-ECO - 4.4.6.2
		Project:	Bibiyana Gas Field Developement
		Tag No.:	

No	Data	Specified	Unit	Opt Avail	Remark
1	**Project/Field Specific Information - Flowing condition at meter location (client input):**				
2	**Ambient Temperature**	TBD	°C		
3	**Minimum flow rate**	2 251 189 (800 MACFD)	Sm3/d		
4	**Nominal flow rate**		Sm3/d		
5	**Maximum flow rate**	2 256 853 (1087 MACFD)	Sm3/d		
6	**Water salinity**	TBD	ppm		
7	**Process Density range**				
8	Oil	680 - 720 (43,5 - 45,1 lb/ft3)	kg/m3		
9	Gas	16 - 64 (1,15 - 4,46 lb/ft3)	kg/m3		
10	**Process % Gas Range**	98,6 - 99,3	%		
11	**Process WLR Range**	25	%		
12	**Process Temperature range**	30 - 40 (87 - 105 °F)	°C		
13	**Process Pressure Range**	48 - 87 (695 - 1265 psig)	barg		
14	**Process and Fluid data**				
15	CO2	0,0024	mol%		
16	H2S	TBD	ppm		
17	Hydrate Formation Temperature	TBD	°C		
18	Sand rate	TBD	ppm		
19	**Process Equip. Design Press/Temp**				
20	Design Pressure	101 (1464 psig)	barg		
21	Design Temperature	66 (150 °F)	°C		
22	**Process Line**				
23	Pipe Schedule	40s			
24	Pipe ID	6"	in		
25	Flange type & rating	6" 600#RTJ			
26	**Meter Operating Ranges:**				
27	**Ambient Temperature**	-10 to 60 (14 - 140 °F)	°C		
28	**Area Classification**	Zone 1, IIB, T5			
29	**Fluid**				
30	Water Salinity	0 - 25	%w/w NaCl		
31	% Gas (GLR) Range	91 - 100	% vol		Note b
32	WLR Range	0 - 100 (0-50 for GLR < 99%)	% vol		
33	**Mechanical Data**				
34	**Design**				
35	***Meter Type***	6" Topside Version			
36	***Hazardous Area Approval***	CENELEC EExde (ia) IIB T5			
37	***dP element***				
38	Type	V-Cone			
39	Beta ratio	0,73			
40	Cone to inner wall gap	23,74 (0,94 in)	mm		
41	Cone diameter	102,52 (4,04 in)	mm		
42	Tap spacing	283,0	mm		Note a
43	***Meter Body Design***				
44	Bore diameter (ID)	150,0 (5.9 in)	mm		
45	Design pressure	101 (1464 psig)	barg		
46	Design temperature	66 (150 °F)	°C		
47	***Meter Body Flange Connection***				
48	Upstream	6" 600# RTJ			
49	Downstream	6" 600#RTJ			
50	***Materials***				
51	Meter Body	Duplex UNS S31803			
52	Microwave Probe	PEEK/Duplex			
53	Thermowell	Provided by Unocal			
54	Instrument Tubing	SS316			

RFM Wet Gas Meter
Topside Version

Serial No.: WGM-1017-05 to WGM-1023-05

roxar
MAXIMUM RESERVOIR PERFORMANCE

INSTRUMENT DATA SHEET

Project no.:	55321003	Customer:	Unocal Bangladesh
Doc No/Rev.:	TCE 005213/B	P.O. No.:	UBBTL-ECO - 4.4.6.2
		Project:	Bibiyana Gas Field Developement
		Tag No.:	

No	Data	Specified		Unit	Opt Avail	Remark
55	lifting lug	Carbon steel, LBG M16				
56	*Protective coating*	In accordance to NORSOK M-501				
57	Coulor	TBA				
58	*Dimension*					
59	Meter Body (face to face)	Estimated to 790		mm		
60	Electronics Enclosure	405 x 663 x 252	(15,94 x 26,10 x 9,92 in)	mm		
61	Coax Cables (Length)	2 x 3.5	(2 x 11,48 ft)	m		
62	*Weight*					
63	Meter Body	TBD		kg		
64	Electronics Enclosure	Estimated to 75		kg		
65	*Ex-e enclosure cable entries*	3 x M20, 2 x M25 and 1 x M32 gland holes				
66	*Mounting*					
67	Meter Body	Inline vertical flow upwards				Note d
68	**Transmitters**					
69	*Densitometer*	NA				
70	*Transmitters*					
71	Hazardous Location Certification	Eexd				
72	Temperature					
73	Number of transmitters	1				
74	Transmitter type	Fisher Rosemount 3144				
75	Interface	HART (digital)				
76	Calibrated Range	0-90		°C		
77	Pressure					
78	Number of transmitters	1				
79	Transmitter type	3051TG4 Emerson				
80	Interface	HART (digital)				
81	Calibrated Range	0-120	(0-1740 psig)	barg		
82	*Delta Pressure*					
83	Number of transmitters	1				
84	Transmitter type	3051CD3 Emerson				
85	Interface	HART (digital)				
86	Calibrated Range	0-2500	(0 - 36,3 psig)	mbar		Note c
87	Max. single side pressure	250	(3626 psig)	barg		
88	Impulse lines	Open line				
89	**Electrical Data**					
90	**Power**					
91	Power Supply in meter	120 VAC, 50 to 60 Hz				
92	Power Consumption	35		W		
93	*Serial Ports*					
94	Number of serial ports	2				
95	Communication protocol	MODBUS RTU				

RFM Wet Gas Meter
Topside Version

INSTRUMENT DATA SHEET

Serial No.: WGM-1017-05 to WGM-1023-05

Project no.:	**55321003**	Customer:	**Unocal Bangladesh**
Doc No/Rev.:	**TCE 005213/B**	P.O. No.:	**UBBTL-ECO - 4.4.6.2**
		Project:	**Bibiyana Gas Field Developement**
		Tag No.:	

No	Data	Specified	Unit	Opt Avail	Remark
96	*Port1*	**RS 485**			
97	Communication addresses	For WGM 1017-05: 21			
		For WGM 1018-05: 22			
		For WGM 1019-05: 23			
		For WGM 1020-05: 24			
		For WGM 1021-05: 25			
		For WGM 1022-05: 26			
		For WGM 1023-05: 27			
98	Settings	**Baud=9600, Data bits=8, Stop bits=2, no parity**			
99	Number of wires	**2**			
100	*Port2*	**RS 485**			
101	Communication addresses	For WGM 1017-05: 211			
		For WGM 1018-05: 212			
		For WGM 1019-05: 213			
		For WGM 1020-05: 214			
		For WGM 1021-05: 215			
		For WGM 1022-05: 216			
		For WGM 1023-05: 217			
102	Settings	**Baud=9600, Data bits=8, Stop bits=2, no parity**			
103	Number of wires	**2**			

No			
104	**NOTES:**		
105	a. RFM internal design parameter		
106	b. Uncertainty specification is valid for GLR range 95 - 100 %vol.		
107	c. Accuracy will be degraded for low diff. pressure. Dp transmitter will measure below low range, accuracy cannot be guaranteed.		
108	d. Blind-T required upstream of meter positioned 2-10 ID of straight piping from Vcone edge/Mw probes.		
109	e.		
110	f.		
111	g.		
112	**OPTIONS:**	**Ordered?**	
113		**Yes**	**No**
114	o1 Simulator for communication testing		X
115	o2 Thermal Insulation		X
116	o3 Formation water detection functionality		X
117	o4 Topside computer with Dacqus software	X	
118	o7 Witnessed FAT, functional flowtest of one unit	X	
119	o8 K-Lab test		X
120	**SPARES:**	**Ordered?**	
121		**Yes**	**No**
122	s1 Coax cables including attenuators	X	
123	s2 Packing, preservation and handling	X	
124	s3 Pressure transmitter		X
125	s4 Delta pressure transmitter		X
126	s5 Temperature transmitter		X
127	**Additional scope of supply**		
128	v1 Mounting stand and sun/rain shield for Flow Computer/electronics enclosure, designed for earthquake zone 3		
129	v2		
130	v3		
131	v4		
132	v5		

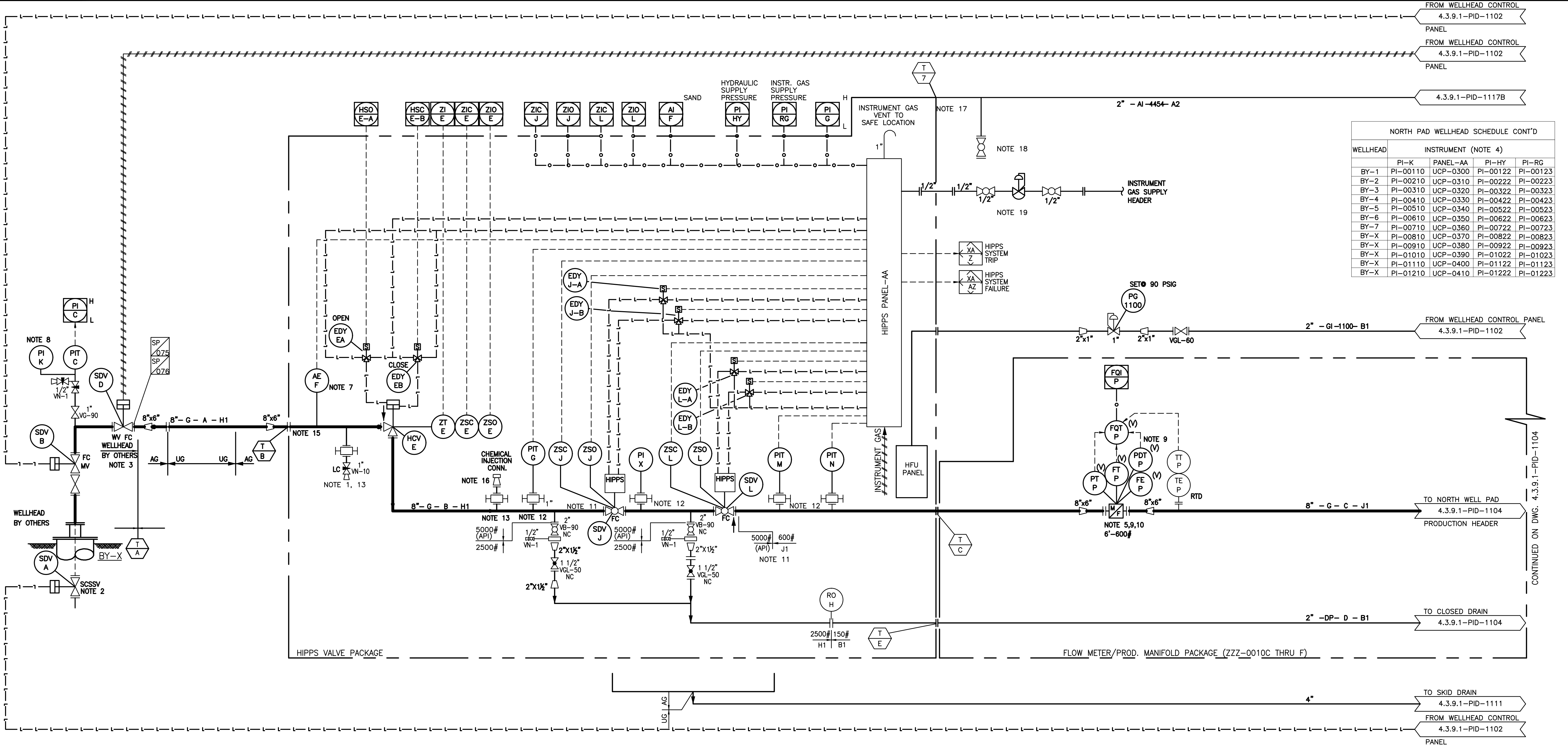

NORTH PAD WELLHEAD SCHEDULE CONT'D

WELLHEAD	INSTRUMENT (NOTE 4)			
	PI-K	PANEL-AA	PI-HY	PI-RG
BY-1	PI-00110	UCP-0300	PI-00122	PI-00123
BY-2	PI-00210	UCP-0310	PI-00222	PI-00223
BY-3	PI-00310	UCP-0320	PI-00322	PI-00323
BY-4	PI-00410	UCP-0330	PI-00422	PI-00423
BY-5	PI-00510	UCP-0340	PI-00522	PI-00523
BY-6	PI-00610	UCP-0350	PI-00622	PI-00623
BY-7	PI-00710	UCP-0360	PI-00722	PI-00723
BY-X	PI-00810	UCP-0370	PI-00822	PI-00823
BY-X	PI-00910	UCP-0380	PI-00922	PI-00923
BY-X	PI-01010	UCP-0390	PI-01022	PI-01023
BY-X	PI-01110	UCP-0400	PI-01122	PI-01123
BY-X	PI-01210	UCP-0410	PI-01222	PI-01223

NORTH PAD WELLHEAD SCHEDULE

INSTRUMENT (NOTE 4)

WELLHEAD	T-A	T-B	T-C	T-E	LINE NUMBER-A	LINE NUMBER-B	LINE NUMBER-C	LINE NUMBER-D	LINE NUMBER-E
BY-1	16	107	452	459	8"-G-1000-H1	8"-G-1012-H1	8"-G-1024-J1	2"-DP-1036-B1	2"-DP-1048-J1
BY-2	21	117	453	460	8"-G-1001-H1	8"-G-1013-H1	8"-G-1025-J1	2"-DP-1037-B1	2"-DP-1049-J1
BY-3	33	121	454	461	8"-G-1002-H1	8"-G-1014-H1	8"-G-1026-J1	2"-DP-1038-B1	2"-DP-1050-J1
BY-4	44	132	455	462	8"-G-1003-H1	8"-G-1015-H1	8"-G-1027-J1	2"-DP-1039-B1	2"-DP-1051-J1
BY-5	54	137	456	463	8"-G-1004-H1	8"-G-1016-H1	8"-G-1028-J1	2"-DP-1040-B1	2"-DP-1052-J1
BY-6	57	165	457	464	8"-G-1005-H1	8"-G-1017-H1	8"-G-1029-J1	2"-DP-1041-B1	2"-DP-1053-J1
BY-7	99	168	458	465	8"-G-1006-H1	8"-G-1018-H1	8"-G-1030-J1	2"-DP-1042-B1	2"-DP-1054-J1
BY-X					8"-G-1007-H1	8"-G-1019-H1	8"-G-1031-J1	2"-DP-1043-B1	2"-DP-1055-J1
BY-X					8"-G-1008-H1	8"-G-1020-H1	8"-G-1032-J1	2"-DP-1044-B1	2"-DP-1056-J1
BY-X					8"-G-1009-H1	8"-G-1021-H1	8"-G-1033-J1	2"-DP-1045-B1	2"-DP-1057-J1
BY-X					8"-G-1010-H1	8"-G-1022-H1	8"-G-1034-J1	2"-DP-1046-B1	2"-DP-1058-J1
BY-X					8"-G-1011-H1	8"-G-1023-H1	8"-G-1035-J1	2"-DP-1047-B1	2"-DP-1059-J1

WELLHEAD	SDV-A	SDV-B	PIT-C	SDV-D	HCV-E	AE-F	PIT-G	RO-H	SDV-J	SDV-L
BY-1	SDV-00101	SDV-00102	PIT-00103	SDV-00104	HCV-00105	AE-00106	PIT-00107	RO-00108	SDV-00109	SDV-00111
BY-2	SDV-00201	SDV-00202	PIT-00203	SDV-00204	HCV-00205	AE-00206	PIT-00207	RO-00208	SDV-00209	SDV-00211
BY-3	SDV-00301	SDV-00302	PIT-00303	SDV-00304	HCV-00305	AE-00306	PIT-00307	RO-00308	SDV-00309	SDV-00311
BY-4	SDV-00401	SDV-00402	PIT-00403	SDV-00404	HCV-00405	AE-00406	PIT-00407	RO-00408	SDV-00409	SDV-00411
BY-5	SDV-00501	SDV-00502	PIT-00503	SDV-00504	HCV-00505	AE-00506	PIT-00507	RO-00508	SDV-00509	SDV-00511
BY-6	SDV-00601	SDV-00602	PIT-00603	SDV-00604	HCV-00605	AE-00606	PIT-00607	RO-00608	SDV-00609	SDV-00611
BY-7	SDV-00701	SDV-00702	PIT-00703	SDV-00704	HCV-00705	AE-00706	PIT-00707	RO-00708	SDV-00709	SDV-00711
BY-X	SDV-00801	SDV-00802	PIT-00803	SDV-00804	HCV-00805	AE-00806	PIT-00807	RO-00808	SDV-00809	SDV-00811
BY-X	SDV-00901	SDV-00902	PIT-00903	SDV-00904	HCV-00905	AE-00906	PIT-00907	RO-00908	SDV-00909	SDV-00911
BY-X	SDV-01001	SDV-01002	PIT-01003	SDV-01004	HCV-01005	AE-01006	PIT-01007	RO-01008	SDV-01009	SDV-01011
BY-X	SDV-01101	SDV-01102	PIT-01103	SDV-01104	HCV-01105	AE-01106	PIT-01107	RO-01108	SDV-01109	SDV-01111
BY-X	SDV-01201	SDV-01202	PIT-01203	SDV-01204	HCV-01205	AE-01206	PIT-01207	RO-01208	SDV-01209	SDV-01211

WELLHEAD	PIT-M	PIT-N	FT-P	PI-U	PI-V	PI-W	PI-X	XA-Z	XA-AZ	ESY-B/D	TE-P
BY-1	PIT-00112	PIT-00113	FQT-00115	PI-00101	PI-00102	PI-00104	PI-00118	XA-00120	XA-00121	ESY-00102	TE-00115
BY-2	PIT-00212	PIT-00213	FQT-00215	PI-00201	PI-00202	PI-00204	PI-00218	XA-00220	XA-00221	ESY-00202	TE-00215
BY-3	PIT-00312	PIT-00313	FQT-00315	PI-00301	PI-00302	PI-00304	PI-00318	XA-00320	XA-00321	ESY-00302	TE-00315
BY-4	PIT-00412	PIT-00413	FQT-00415	PI-00401	PI-00402	PI-00404	PI-00418	XA-00420	XA-00421	ESY-00402	TE-00415
BY-5	PIT-00512	PIT-00513	FQT-00515	PI-00501	PI-00502	PI-00504	PI-00518	XA-00520	XA-00521	ESY-00502	TE-00515
BY-6	PIT-00612	PIT-00613	FQT-00615	PI-00601	PI-00602	PI-00604	PI-00618	XA-00620	XA-00621	ESY-00602	TE-00615
BY-7	PIT-00712	PIT-00713	FQT-00715	PI-00701	PI-00702	PI-00704	PI-00718	XA-00720	XA-00721	ESY-00702	TE-00715
BY-X	PIT-00812	PIT-00813	FQT-00815	PI-00801	PI-00802	PI-00804	PI-00818	XA-00820	XA-00821	ESY-00802	
BY-X	PIT-00912	PIT-00913	FQT-00915	PI-00901	PI-00902	PI-00904	PI-00918	XA-00920	XA-00921	ESY-00902	
BY-X	PIT-01012	PIT-01013	FQT-01015	PI-01001	PI-01002	PI-01004	PI-01018	XA-01020	XA-01021	ESY-01002	
BY-X	PIT-01112	PIT-01113	FQT-01115	PI-01101	PI-01102	PI-01104	PI-01118	XA-01120	XA-01121	ESY-01102	
BY-X	PIT-01212	PIT-01213	FQT-01215	PI-01201	PI-01202	PI-01204	PI-01218	XA-01220	XA-01221	ESY-01202	

NOTE 6

NOTES

1. CONNECTION FOR METHANOL INJECTION
2. TIME DELAY IN WHCP TO ENSURE SCSSV CLOSES AFTER MV & WV. SCSSV MUST BE OPENED BEFORE MV & WV TO PREVENT HIGH DIFFERENTIAL PRESSURE ACROSS VALVE
3. 5 1/8"- 5000 LB., API TYPE 6B WELDING NECK COMPANION FLANGE SUPPLIED BY OTHERS.
4. SEE DWG. NO. 4.3.9.1-PID-1102 FOR WELLHEAD CONTROL PANELS.
5. MULTIPHASE FLOW METERS TO BE INSTALLED IN VERTICAL POSITION WITH FLOW IN UPWARD DIRECTION.
6. DELETED.
7. CLAMP-ON PIPE ULTRASONIC SAND DETECTOR.
8. DRILLING WILL PROVIDE A LOCAL PI. PROJECT SHALL PROVIDE PRESSURE TRANSMITTER.
9. METER TO BE SUPPLIED BY OWNER AND INSTALLED PRIOR TO COMMISSIONING.(V)
10. SKID SUPPLIER TO INSTALL PIPE SPOOL IN LIEU OF FLOW METER.
11. 5000# PIPING SPEC WITH "GREYLOK" FLANGES.
12. 2500# RTJ 2 VALVE MONOFLANGE.
13. 2500# RTJ BLOCK VALVE MONOFLANGE.
14. VENT ALL SDV'S AND CONTROL VALVE ACTUATORS OPERATING WITH INSTRUMENT GAS TO A SAFE LOCATION.
15. ISOLATING 5000# "GREYLOK" FLANGE.
16. 1" x 1/2" TUBING CONNECTION WITH CAP
17. FOR "HIPPS PANEL-AA" PURGE CONNECTION.
18, ONLY FOR FUTURE CONNECTION.
19. SCOPE OF INSTALLATION UNDER MOC-BY-09-007

REFERENCE	NUMBER	NO.	DATE	REVISION	BY	CHK	APPR	APPR
-	-	4	25 AUG,11	ISSUED FOR CHANGE UNDER SOW OF MOC-BY-09-007	SJRG	HISL	LMOY	JWLO
-	-	3	18 JAN'10	AS-BUILT	SA	IFTE	AH	DO
-	-	2	7 MAR'08	ISSUED FOR FIELD VERIFICATION	SPK	JLL	PM	RS
-	-	1	18-FEB-06	RE-ISSUED FORUSE	IMA	IMA	IMA	MBC
-	-	0	15-NOV-05	ISSUED FOR USE	BTE	BTE	IMA	MBC
-	-	C	25-JUN-05	ISSUED FORDESIGN	BTE	EF	IMA	JCW
-	-	B	25-MAY-05	ISSUED FOR HAZOP	OL	EF	IMA	JCW
-	-	A1	21-APR-05	ISSUED FOR PACKAGE BID	OL	EF	IMA	
-	-	A	21-MAR-05	FOR INTERNAL REVIEW	KJN	CF	IMA	

WorleyParsons

Chevron Bangladesh

DRAWING APPROVALS

DRAWN:	WPG	DATE:
CHECKED:		DATE:
ENGINEER:		DATE:
W.Parsons:		DATE:

BIBIYANA GAS PLANT
TYPICAL WELLHEAD
NORTH WELL PAD
PIPING & INSTRUMENT DIAGRAM

SCALE	PROJECT NO.	DRAWING NO.	REV.
NONE	15632501	4.3.9.1-PID-1100	4

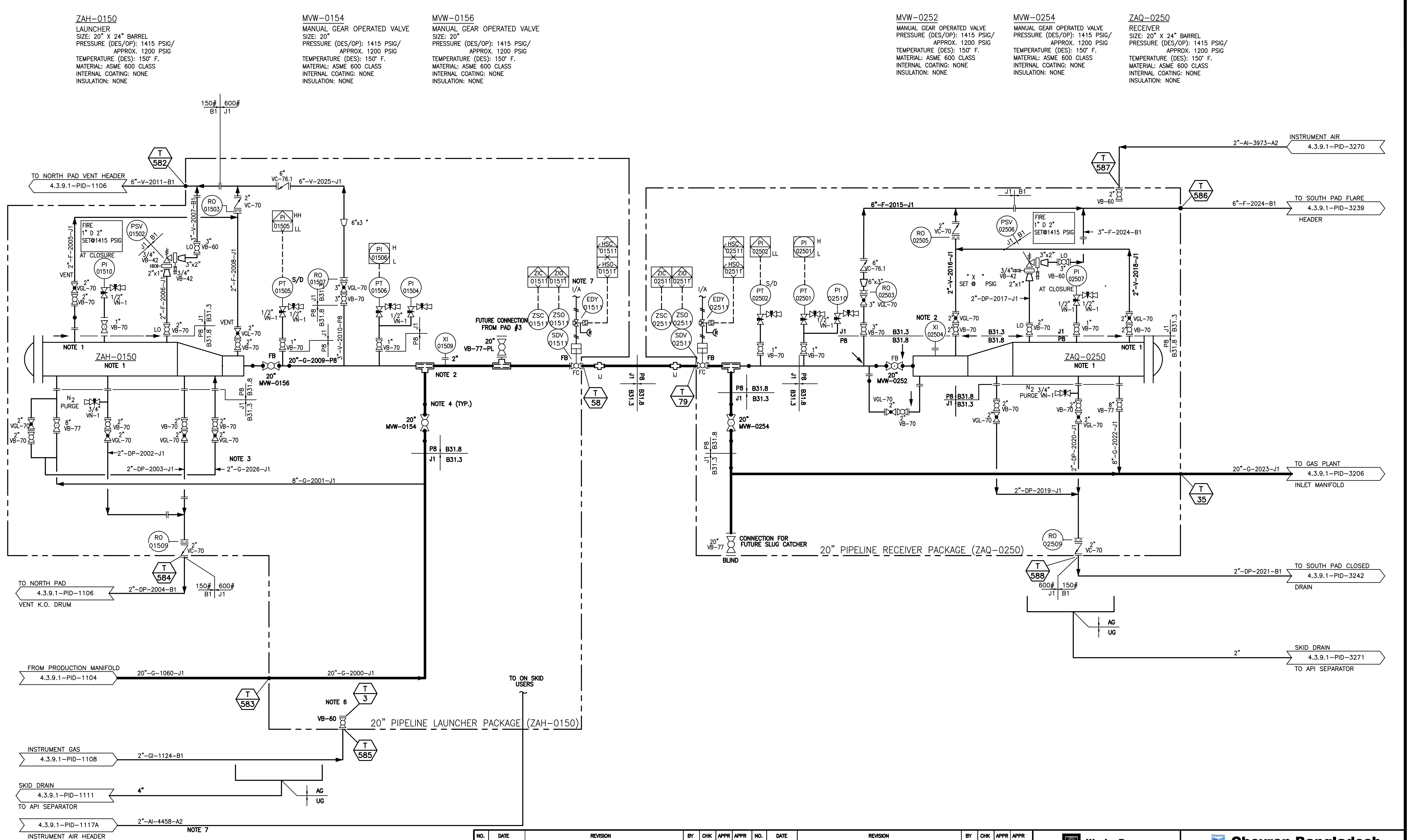

NOTES
1. LAUNCHER AND RECEIVER TO BE PROVIDED WITH QUICK OPENING PRESSURE WARNING DEVICE TO PREVENT OPENING UNDER PRESSURE.
2. PIG SIGNALER
3. PRESSURE EQUALIZING LINE.
4. WELD POINTS.
5. VENT ALL SDV'S AND CONTROL VALVE ACTUATORS OPERATING WITH INSTRUMENT GAS TO A SAFE LOCATION.
6. INSTRUMENT AIR LINE ISOLATED AND BLINDED.
7. SCOPE OF INSTALLATION UNDER MOC-BY-09-020

NO.	DATE	REVISION	BY	CHK	APPR	APPR	NO.	DATE	REVISION	BY	CHK	APPR	APPR
5	21 AUG,11	ISSUED FOR CHANGE UNDER SOW OF MOC-BY-09-020	SJRG	HISL	LMOY	JWLO	4	18 JAN'10	AS-BUILT	SA	IFTE	AH	DO
							3	7 MAR'08	ISSUED FOR FIELD VERIFICATION	SLR	JLL	PM	RS
							2	31-AUG-06	REISSUED FOR USE	IMA	IMA	IMA	MBC
							1	16-FEB-06	RE-ISSUED FOR USE	IMA	IMA	IMA	MBC
							0	15-NOV-05	ISSUED FOR USE	BTE	IMA	IMA	MBC
							D	15-SEP-05	REISSUED FOR DESIGN PER DCN	BTE	BTE	IMA	MBC
							C	24 JUN-05	ISSUED FOR DESIGN	BTE	EF	IMA	JCW
							B	18-MAY-05	ISSUED FOR HAZOP	EF	EF	IMA	JCW
							A1	5-MAY-05	ISSUED FOR PACKAGE BID	KJN	EF	IMA	

WorleyParsons

Chevron Bangladesh

DRAWING APPROVALS

DRAWN:	WPG	DATE:	15-MAR-05
CHECKED:		DATE:	
ENGINEER:		DATE:	
W.Parsons:		DATE:	

BIBIYANA GAS PLANT
20" GAS GATHERING PIPELINE
(NORTH PAD TO SOUTH PAD)
PIPING & INSTRUMENT DIAGRAM

SCALE	PROJECT NO.	DRAWING NO.	REV.
N.T.S.	15632501	4.3.9.1-PID-2107	5

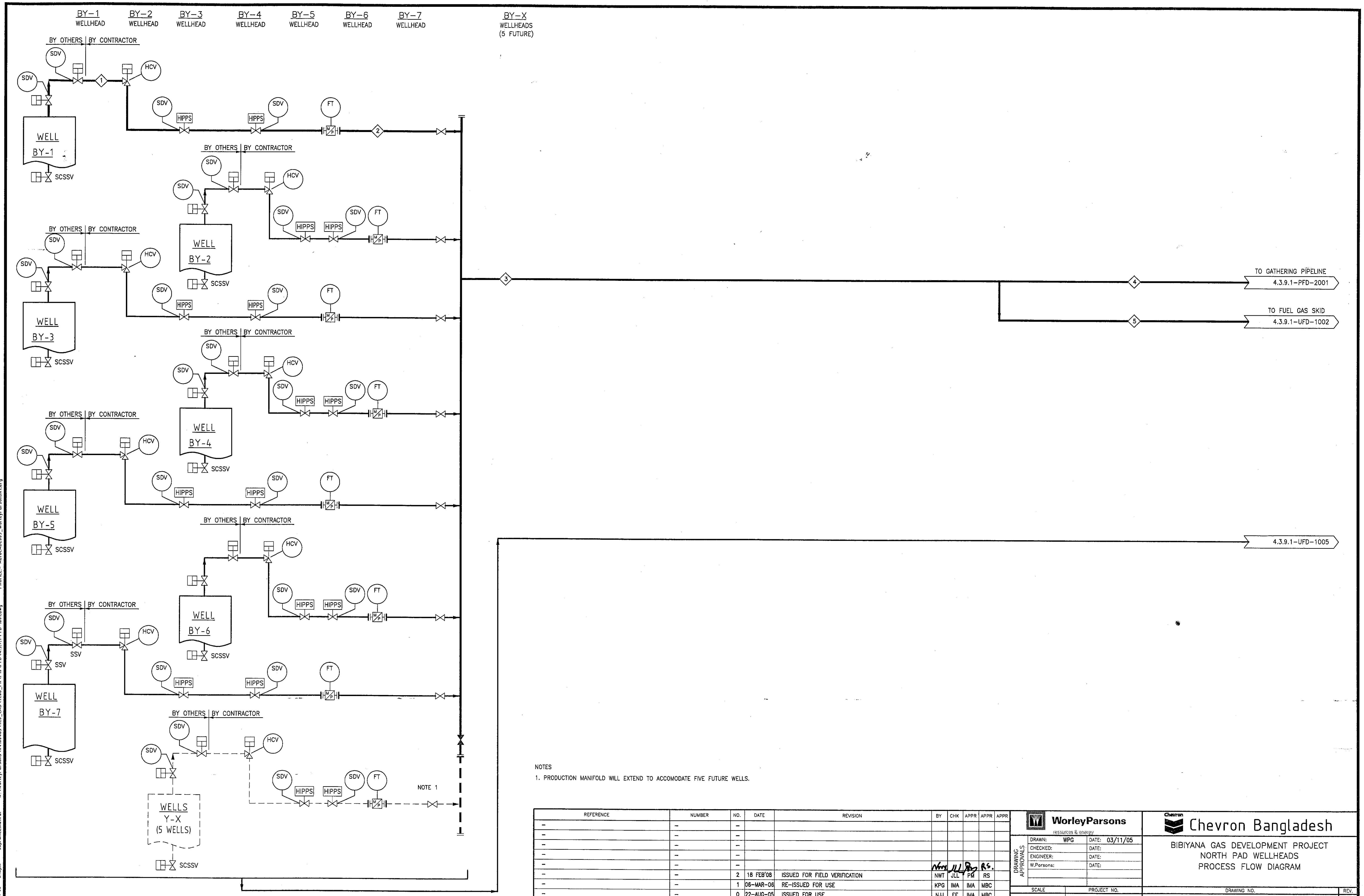

NOTES

1. PRODUCTION MANIFOLD WILL EXTEND TO ACCOMODATE FIVE FUTURE WELLS.

REFERENCE	NUMBER	NO.	DATE	REVISION	BY	CHK	APPR	APPR	APPR
–	–	–							
–	–	–							
–	–	–							
–	–	–							
–	–	–			Nwt	JLL	PM	RS.	
–	–	2	18 FEB'08	ISSUED FOR FIELD VERIFICATION	NWT	JLL	PM	RS	
–	–	1	06-MAR-06	RE-ISSUED FOR USE	KPG	IMA	IMA	MBC	
–	–	0	22-AUG-05	ISSUED FOR USE	NJJ	EF	IMA	MBC	
–	–	A	17-MAR-05	ISSUED FOR INTERNAL REVIEW					

WorleyParsons
resources & energy

DRAWING APPROVALS		
DRAWN:	WPG	DATE: 03/11/05
CHECKED:		DATE:
ENGINEER:		DATE:
W.Parsons:		DATE:

Chevron

Chevron Bangladesh

BIBIYANA GAS DEVELOPMENT PROJECT
NORTH PAD WELLHEADS
PROCESS FLOW DIAGRAM

SCALE	PROJECT NO.	DRAWING NO.	REV.
N.T.S.	15632501	4.3.9.1-PFD-1001	2